Article

Cell Host & Microbe

Dietary Fructose and Microbiota-Derived Short-Chain Fatty Acids Promote Bacteriophage Production in the Gut Symbiont *Lactobacillus reuteri*

Graphical Abstract

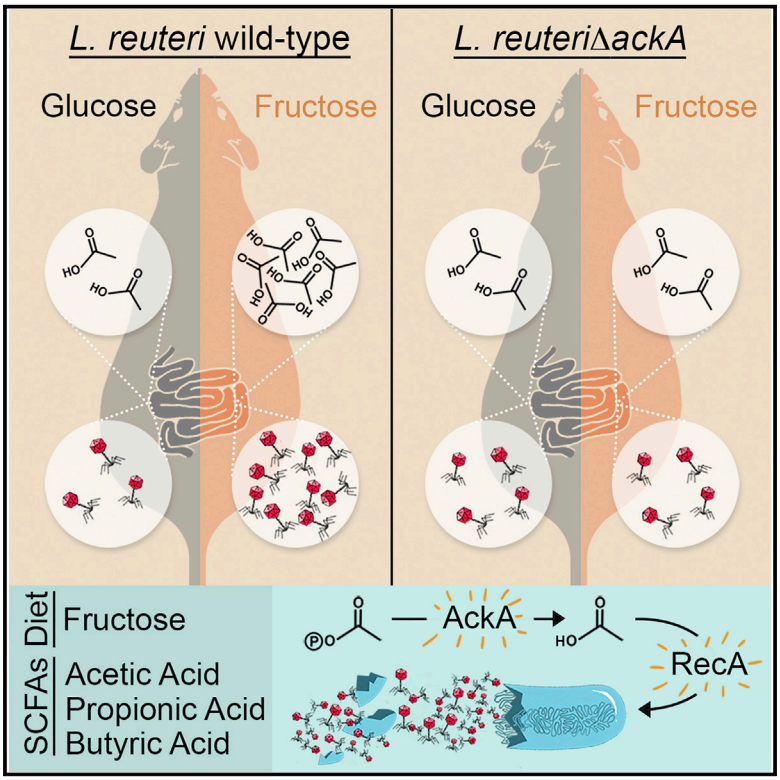

Highlights

- *Lactobacillus reuteri* produces phage during gastrointestinal transit
- Dietary fructose and SCFAs promote *L. reuteri* phage production
- Fructose metabolism and SCFA exposure activate the Ack pathway
- The Ack pathway promotes phage production in a RecA-dependent manner

Authors

Jee-Hwan Oh, Laura M. Alexander, Meichen Pan, ..., Alan D. Attie, Jens Walter, Jan-Peter van Pijkeren

Correspondence

vanpijkeren@wisc.edu

In Brief

Oh et al. discover that the central carbon metabolism of the gut symbiont *Lactobacillus reuteri* is intimately connected to phage production. Dietary fructose or exposure to SCFAs activates the Ack pathway in *Lactobacillus reuteri*, which evokes a global stress response in the bacterium that consequently leads to increased phage production.

Oh et al., 2019, Cell Host & Microbe *25*, 1–12
February 13, 2019
https://doi.org/10.1016/j.chom.2018.11.016

CellPress

Please cite this article in press as: Oh et al., Dietary Fructose and Microbiota-Derived Short-Chain Fatty Acids Promote Bacteriophage Production in the Gut Symbiont *Lactobacillus reuteri*, Cell Host & Microbe (2018), https://doi.org/10.1016/j.chom.2018.11.016

Cell Host & Microbe
Article

Dietary Fructose and Microbiota-Derived Short-Chain Fatty Acids Promote Bacteriophage Production in the Gut Symbiont *Lactobacillus reuteri*

Jee-Hwan Oh,[1] Laura M. Alexander,[1] Meichen Pan,[1] Kathryn L. Schueler,[2] Mark P. Keller,[2] Alan D. Attie,[2] Jens Walter,[3,4] and Jan-Peter van Pijkeren[1,5,*]
[1]Department of Food Science, University of Wisconsin-Madison, Madison, WI 53706, USA
[2]Department of Biochemistry, University of Wisconsin-Madison, Madison, WI 53706, USA
[3]Department of Agriculture, Food and Nutritional Science, University of Alberta, Edmonton, AB T6G 2P5, Canada
[4]Department of Biological Sciences, University of Alberta, Edmonton, AB T6G 2P5, Canada
[5]Lead Contact
*Correspondence: vanpijkeren@wisc.edu
https://doi.org/10.1016/j.chom.2018.11.016

SUMMARY

The mammalian intestinal tract contains a complex microbial ecosystem with many lysogens, which are bacteria containing dormant phages (prophages) inserted within their genomes. Approximately half of intestinal viruses are derived from lysogens, suggesting that these bacteria encounter triggers that promote phage production. We show that prophages of the gut symbiont *Lactobacillus reuteri* are activated during gastrointestinal transit and that phage production is further increased in response to a fructose-enriched diet. Fructose and exposure to short-chain fatty acids activate the Ack pathway, involved in generating acetic acid, which in turn triggers the bacterial stress response that promotes phage production. *L. reuteri* mutants of the Ack pathway or RecA, a stress response component, exhibit decreased phage production. Thus, prophages in a gut symbiont can be induced by diet and metabolites affected by diet, which provides a potential mechanistic explanation for the effects of diet on the intestinal phage community.

INTRODUCTION

The human gastrointestinal (GI) tract harbors a complex community of microorganisms, composed of bacteria, archaea, protozoa, and fungi (Ley et al., 2008; Yatsunenko et al., 2012). Most human-associated microbes are bacteria, of which many contain prophages—viral DNA that originates from temperate bacteriophages (phages) that have integrated into their genome (Breitbart et al., 2003). Prophages can be activated under specific conditions, leading to the excision of the DNA and formation of active phages, which are released in the ecosystem. The human gut contains more virus-like particles than bacteria, and several lines of evidence suggest that most virus-like particles are derived from prophages rather than lytic phages (Breitbart et al., 2003; Reyes et al., 2012; Howe et al., 2016).

Despite numerical dominance of prophages in the gut, most knowledge on phages in the gut ecosystem resulted from metagenomic studies that can only generate hypotheses in regard to mechanisms of phage induction (Minot et al., 2011; Kleiner et al., 2015; Manrique et al., 2016). Few studies have focused on prophages in gut bacteria, and those that did relied mostly on genome comparisons (Canchaya et al., 2003). More recently, associations have been made between gut inflammation and the production of phages, which shows that changes in the gut environment drive phage production (Diard et al., 2017; Cornuault et al., 2018; Duerkop et al., 2018). However, little is known to what extent the gut phageome is influenced by the ecological conditions in the healthy gut.

Research studying the impact of diet on the gut ecosystem has mostly focused on the bacterial community, which can be altered rapidly in a diet-specific manner; however, changes are temporal and community composition reverts to the original state after the dietary modulation ends (Martínez et al., 2010; David et al., 2013). So far, few studies have included the gut virome in the analysis despite emerging evidence that diet also influences the phageome. Clearly, such changes could just be the consequence of the shifts in the abundance of the bacterial hosts (Minot et al., 2011). However, both the magnitude and duration by which the phageome shifts in response to diet appears to exceed what has been observed for diet-induced shifts in the bacterial community (Minot et al., 2011). In fact, one study shows that the phageome community did not recover during the washout period after a diet enriched in refined sugars, suggesting longer-term consequences of a diet with increased sugar intake (Howe et al., 2016). As of today, we have no mechanistic understanding of how diet induces such profound alterations in the phageome, but preliminary data suggest a contribution of prophage induction (Minot et al., 2011). The objective of our work was to test the hypothesis that diet induces metabolic changes in a lysogen that can activate prophages in the gut.

Lactobacillus reuteri is a bacterial gut symbiont found in the digestive tract of many vertebrate hosts, including humans, pigs, cattle, rodents, sheep, and birds (Duar et al., 2017). *L. reuteri* modulates the host immune system by tryptophan metabolism to yield

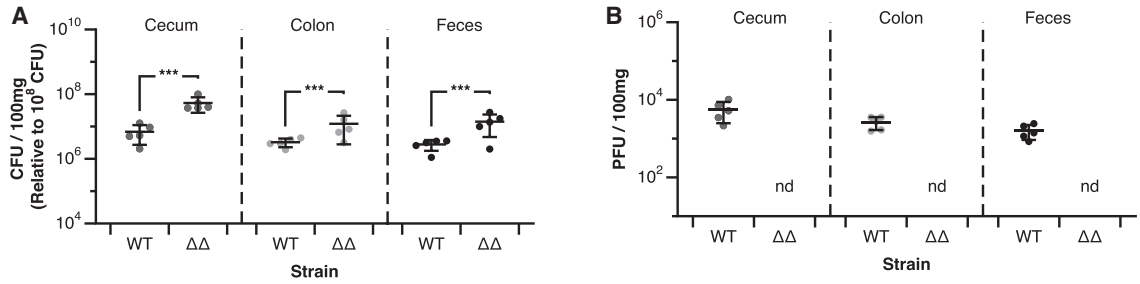

Figure 1. Prophages of *L. reuteri* 6475 Are Activated during Gastrointestinal Transit and Reduce Survival

(A) Cell numbers of *L. reuteri* 6475 wild-type (WT) and *L. reuteri* 6475ΔΦ1ΔΦ2 (ΔΔ) determined by bacterial culture from cecum, colon, and feces. Data are expressed per 100 mg content and normalized to 10^8 administered CFU. ***$p < 0.001$.

(B) Phage numbers expressed as plaque-forming units (PFU) per 100 mg cecal, colonic, and fecal content derived from mice administered WT or ΔΔ. n = 5 animals/group; nd, not detected.

indole derivatives that activate the aryl-hydrocarbon receptor, a transcription factor that plays a role in reducing intestinal inflammation and metabolic syndrome (Zelante et al., 2013; Natividad et al., 2018). Select strains of *L. reuteri* also prevent bone loss in women with low bone-mineral density (Nilsson et al., 2018). *L. reuteri* can utilize a wide range of monosaccharide and disaccharide sugars, and like other obligate heterofermentative lactobacilli, *L. reuteri* uses the 6-phosphogluconate/phosphoketolase (6-PG/PK) pathway to produce lactic acid together with ethanol and/or acetic acid (Kandler et al., 1980; Zheng et al., 2015).

In the context of studying the role of diet on phage production, fructose is of special interest. First, fructose metabolism by *L. reuteri* alters the metabolic flux in the cells, thereby increasing production of the short-chain fatty acid (SCFA) acetic acid by *L. reuteri*. Fructose can function as an electron acceptor to be metabolized to mannitol with concomitant oxidation of NADH to NAD^+. The key intermediate in the PK pathway is acetyl-P, which is converted to ethanol to regenerate reduced co-factors, or—if alternative electron acceptors such as fructose are available—to acetic acid by the enzyme acetate kinase (AckA) (Rodriguez et al., 2012). Second, fructose consumption in humans has dramatically increased. In the late 1960s, high-fructose corn syrup was developed, which in the United States was introduced to foods and beverages in the early 1970s. Since 1970, the average fructose consumption has increased 4-fold (Johnson et al., 2007). Consequently, in today's diet fructose accounts for approximately 10% of the caloric intake (Vos et al., 2008). Despite its importance, the impact of dietary fructose on phage production in the gut has not been studied to date.

In this study, we developed *L. reuteri* 6475 as a model to understand the impact of sugar metabolism on phage production. We unraveled the molecular underpinnings that drive phage production in the gut as a consequence of fructose metabolism and exposure to SCFAs. Collectively, our findings provide a potential mechanistic explanation for the impact of diet on the phageome in the gut.

RESULTS

Development of *L. reuteri* 6475 as a Platform to Study Prophages in a Gut Symbiont

The genome content of *L. reuteri* 6475 is highly similar to that of *L. reuteri* JCM1112^T (Walter et al., 2011), a type strain for which a closed genome is available. Using JCM1112^T as a reference genome, we identified two prophage genomes in strain *L. reuteri* 6475: LRΦ1 (43.3 kb) and LRΦ2 (43.7 kb). These genomes contain well-defined conserved modules responsible for DNA integration, regulation, DNA packaging, and head and tail morphogenesis, and the gene order is typical for Siphoviridae phages (Hatfull, 2008). Prophage induction with the chemical inducer mitomycin C reduced the cell density, which is indicative of lysis (Figure S1A). The prophages have unique *attB* sites, and PCR analyses revealed that each prophage can be excised (Figures S1B and S1C).

To understand the biological role of *L. reuteri* 6475 prophages, we used a recently developed counter-selection system (Zhang et al., 2018) to delete the prophages and their *attB* sites, after which we restored the *attB* sites, resulting in strain *L. reuteri*ΔΦ1ΔΦ2 (see STAR Methods). While this strain becomes a lysogen when exposed to phages, we found that one of the intermediate strains lacking the *attB* sites, *L. reuteri*ΔΦ1ΔΦ2*ΔattB1ΔattB2*, formed plaques upon the addition of LRΦ1 or LRΦ2. This allowed us to use *L. reuteri*ΔΦ1ΔΦ2*ΔattB1ΔattB2* as a sensitive host to enumerate plaque-forming units (PFU). Collectively, we developed isogenic mutants of the gut symbiont *L. reuteri* 6475 to study its prophages.

L. reuteri 6475 Prophages Are Activated during Gastrointestinal Transit and Reduce Fitness of Their Host

To assess whether *L. reuteri* 6475 prophages are of relevance during GI transit, we determined survival of *L. reuteri* wild-type and *L. reuteri*ΔΦ1ΔΦ2 in the cecum, colon, and feces after oral administration. Our results showed that prophages reduced survival: we recovered from the cecum, colon, and feces respectively 7.8-, 3.7-, and 5-fold less *L. reuteri* wild-type compared with *L. reuteri*ΔΦ1ΔΦ2 ($p < 0.001$) (Figure 1A). When we examined phage production, we detected on average 5.6×10^3, 2.6×10^3 and 1.6×10^3 PFU in the cecum, colon, and feces, respectively, when animals were administered *L. reuteri* wild-type (Figure 1B). No plaques were recovered from animals upon administration of *L. reuteri*ΔΦ1ΔΦ2. Thus, during GI transit the survival of *L. reuteri* 6475 is reduced as a consequence of phage production.

To understand the distribution of phages produced during GI transit, we performed plaque assays with *L. reuteri*ΔΦ2 *ΔattB2*—a host specific for LRΦ2 and not for LRΦ1. We did

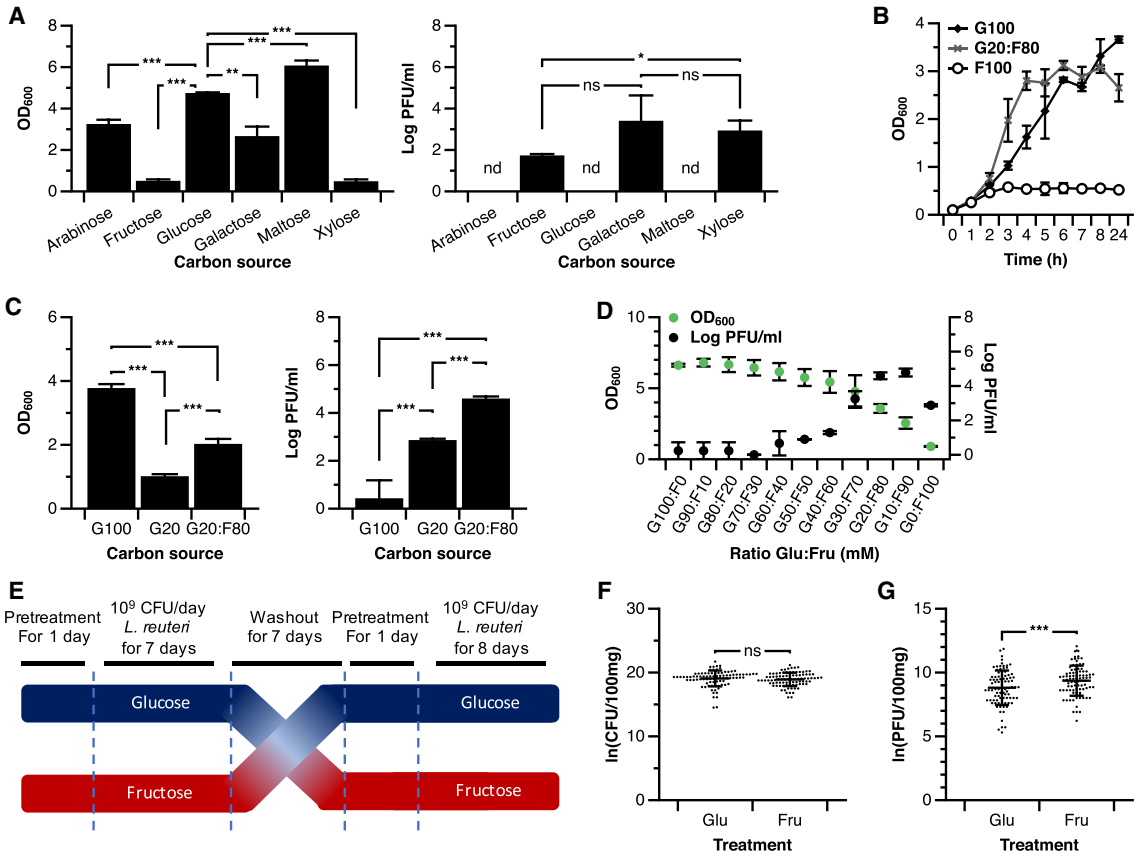

Figure 2. Fructose Metabolism Increases Phage Production in *L. reuteri* 6475

(A) Cell density of *L. reuteri* (left panel) and phage production (right panel) upon 24 hr growth in mMRS supplemented with different carbon sources. Ns, no statistical significance ($p > 0.05$); nd, not detected; *$p < 0.05$; **$p < 0.01$; ***$p < 0.001$.

(B) Growth of *L. reuteri* in mMRS supplemented with different carbon sources. G100, 100 mM glucose; G20:F80, 20 mM glucose and 80 mM fructose; F100, 100 mM fructose.

(C) *L. reuteri* cell density (left panel) and phage production (right panel) upon 24 hr growth. G100, 100 mM glucose; G20, 20 mM glucose; G20:F80, 20 mM glucose and 80 mM fructose. ***$p < 0.001$.

(D) *L. reuteri* cell density (green, primary y axis) and phage production (black, secondary y axis) after 24 hr growth in mMRS supplemented with a total concentration of 100 mM carbon source consisting of different ratios (mM) of glucose (G) and fructose (F).

(E) Experimental setup for the two-arm dietary crossover study (n = 6 mice/group). Glucose or fructose was added to the drinking water. See STAR Methods for details.

(F and G) Recovery of *L. reuteri* (F) and phage (G) from feces, normalized to 100 mg content, during the crossover study from animals supplemented with glucose (Glu) or fructose (Fru). Each dot represents a single data point from a single mouse on one day. Mice were sampled daily when administered *L. reuteri* and sugar water. The horizontal bars represent means and SD. Data are expressed as the natural log (ln) of CFU or PFU. ns, no statistical significance ($p > 0.05$); ***$p < 0.001$. Data were analyzed with the linear mixed-effects model with repeated measures.

Data in (A) to (D) are presented as means ± SD and are based on three biological replicates. See also Figure S2.

not recover PFU following a plaque assay with the fecal and intestinal contents, which suggests that LRΦ1 is predominantly produced during GI transit in mice fed a conventional chow diet.

Select Monosaccharides Promote Phage Production by *L. reuteri* 6475

Since simple sugars can alter the gut phageome (Howe et al., 2016), we first assessed to what extent *L. reuteri* sugar metabolism affects phage production *in vitro*. We found that arabinose, glucose, galactose, and maltose support growth of *L. reuteri* 6475, while fructose and xylose only marginally increased the optical cell density (Figure 2A, left panel). *L. reuteri* produced phages in media containing galactose, xylose, and fructose (Figure 2A, right panel). Since fructose is one of the most abundant sugars in the Western diet, which, when consumed in adequate amounts, becomes accessible to the microbiota in the colon of mice (Jang et al., 2018), we aimed to obtain a deeper understanding of fructose-mediated phage production by *L. reuteri*.

Fructose Metabolism Increases Phage Production by *L. reuteri* 6475 *In Vivo*

We first assessed the potential of *L. reuteri* 6475 to utilize fructose. *L. reuteri* ATCC 55730—a human isolate located in a different phylogenetic clade than *L. reuteri* 6475 (Oh et al., 2010)—cannot utilize fructose as a carbon source; however,

fructose serves as an electron acceptor to yield additional ATP, and promotes growth when combined with low levels of glucose (Arsköld et al., 2008). We observed also that *L. reuteri* 6475 cannot utilize fructose a sole carbon source (Figure 2B). The small increase in the OD_{600} in the period t = 0–3 hr can most likely be attributed to the carbohydrates present in yeast extract; the growth pattern of *L. reuteri* 6475 was identical in modified deMan Rogosa Sharpe medium (mMRS) (see STAR Methods) that lacked or contained fructose (Figure S2).

When we mixed 20 mM glucose with 80 mM fructose, the growth rate in the logarithmic phase was increased (μ_{max} $0.88_{G20:F80}$ versus 0.45_{G100}) yet the final cell density was lower compared with growth in 100 mM glucose (OD_{600} $2.7_{G20:F80}$ versus 3.7_{G100}, p = 0.004) (Figure 2B). When we assessed phage production, few PFU were identified upon growth in mMRS with 100 mM glucose, while growth under nutrient-limiting conditions (20 mM glucose) boosted phage production 100-fold, yielding 4×10^2 PFU/mL. The combination of 20 mM glucose and 80 mM fructose yielded approximately 4×10^4 PFU/mL (Figure 2C). Thus, fructose metabolism appears to contribute to phage production by *L. reuteri* 6475.

To gain an understanding of the dynamics by which fructose metabolism contributes to phage production, we performed *in vitro* studies with 100 mM carbon source representing different ratios of glucose/fructose. Compared with growth in 100 mM glucose, phage production was not affected within the range of glucose/fructose ratios from 90:10 to 60:40 but was increased to 45 PFU/mL when the host bacteria were cultured in a ratio of 40:60 or higher (Figure 2D). Compared with 100 mM glucose, a glucose/fructose ratio of 20:80 or 10:90 mM increased phage production 10,000-fold yielding approximately 10^5 PFU/mL. Collectively, these data show that fructose metabolism drives *L. reuteri* phage production, which is positively correlated with fructose availability.

Next, we asked to what extent dietary supplementation of fructose affects *L. reuteri* phage production in the gut, and performed a two-phase dietary crossover study in mice (Figure 2E). For 8 consecutive days, mice were supplemented with either fructose or, as a control, glucose in their drinking water to yield an approximate intake of 2 g per kg body weight. The fructose levels are roughly equivalent to high fructose intake of humans and are comparable with those of previous studies (Vos et al., 2008; Jang et al., 2018). At day 2, all animals received *L. reuteri* 6475 for 7 consecutive days. For the second phase, the treatments (glucose or fructose) were reversed after a washout period, and *L. reuteri* was given as described above. No differences in weight gain or loss were observed between the treatment groups (p = 0.547). When compared with glucose, supplementation of fructose yielded a non-significant reduction in *L. reuteri* ($3.3 \times 10^8_{GLU}$ versus $2.7 \times 10^8_{FRU}$ colony-forming units (CFU)/100 mg feces; p = 0.23), while we recovered 1.5-fold more phage ($1.5 \times 10^4_{GLU}$ versus $2.2 \times 10^4_{FRU}$ PFU/100 mg feces; p < 0.0001) (Figures 2F and 2G). Thus, dietary fructose induces phage production of *L. reuteri* in the GI tract.

AckA Drives Fructose-Mediated Phage Production

To understand the mechanism by which fructose drives *L. reuteri* 6475 phage production, we first outlined the predicted pathway of the central carbon metabolism (Figure 3A). Our *in silico* analyses revealed that the enzyme fructokinase is a pseudogene (enzyme 21), while *L. reuteri* 6475 lacks the enzyme phosphofructokinase (enzyme 23). This finding explains why *L. reuteri* 6475 cannot utilize fructose as a substrate for growth, and that the enzyme mannitol dehydrogenase (Mdh; enzyme 20) is solely responsible for fructose metabolism. To test this, we inactivated *mdh*: in glucose medium, growth and glucose consumption were similar to those of the wild-type strain; however, the growth rate was reduced in medium containing 20:80 mM glucose/fructose (Figure S3A). Also, *L. reuteriΔmdh* did metabolize glucose (Figure S3B) but not fructose (Figure S3C) and did not produce acetic acid (Figure S3D), and phage production was not increased upon growth in medium with 20 mM glucose and 80 mM fructose (Figure S3E). We excluded a direct role of mannitol on *L. reuteri* phage production as similar PFU/mL were obtained in medium containing different ratios of glucose and mannitol compared with medium harboring only glucose (Figure S4A), while no acetic acid was produced (Figure S4B).

To determine the metabolic consequences of glucose and fructose metabolism in *L. reuteri* 6475, we quantified glucose and fructose utilization (Figures 3B and 3C), and the metabolic end products upon growth in media containing glucose, fructose, or a mixture of glucose and fructose (Figures 3D–3G). Glucose metabolism yielded lactic acid (Figures 3D and 3E) and ethanol (Figure 3F) as final end products, but no acetic acid (Figure 3G). However, growth in a mixture of glucose and fructose changed the metabolic outcome, shutting down ethanol production and, after 4 hr, conversion of D/L-lactic acid to pyruvate. Acetic acid production steeply increased in the first 4 hr but was produced at a lower rate afterward (Figure 3G). To better understand the dynamics of acetic acid production, we analyzed different glucose/fructose ratios: reducing glucose and increasing fructose gradually increased acetic acid production (Figure 3H), which showed a strong association with phage production (Figure 3I, Pearson's r = 0.88, p < 0.001).

We next asked whether acetic acid production by *L. reuteri* induces phage production. Based on our *in silico* analyses, there can be two routes by which acetic acid can be generated in *L. reuteri* 6475: first, via the Ack pathway that converts acetyl-P to acetic acid (Figure 3A, AckA, enzyme #13); second, via the NAD^+-dependent acetaldehyde dehydrogenase pathway (Figure 3A, enzymes #15 and #16). *L. reuteri* 6475 cannot produce acetic acid from citric acid utilization: *L. reuteri* lacks the enzyme citric acid lyase, which converts citric acid to equimolar levels of acetic acid and oxaloacetic acid. This is of relevance because the growth medium contains citric acid.

To further investigate the role of AckA in acetic acid production, we inactivated *ackA* to generate *L. reuteriΔackA*. In medium containing glucose as the sole carbon source, *L. reuteriΔackA* had a similar growth pattern compared with *L. reuteri* wild-type (Figure 4A). However, in 20:80 mM glucose/fructose, growth of *L. reuteriΔackA* was impaired (μ_{max} 0.88_{WT} versus $0.11_{\Delta ackA}$, p = 0.00015; OD_{600} at 24 hr = $1.74_{\Delta ackA}$ versus 2.62_{WT}; p = 0.0063) (Figure 4B), and—compared with the wild-type—acetic acid production was delayed and reduced, but not completely abolished (Figure 4C).

We complemented *L. reuteriΔackA* by placing *ackA* under the control of an inducible promoter to yield pSIP-*ackA* (COMP), which restored growth and acetic acid production (Figures 4D

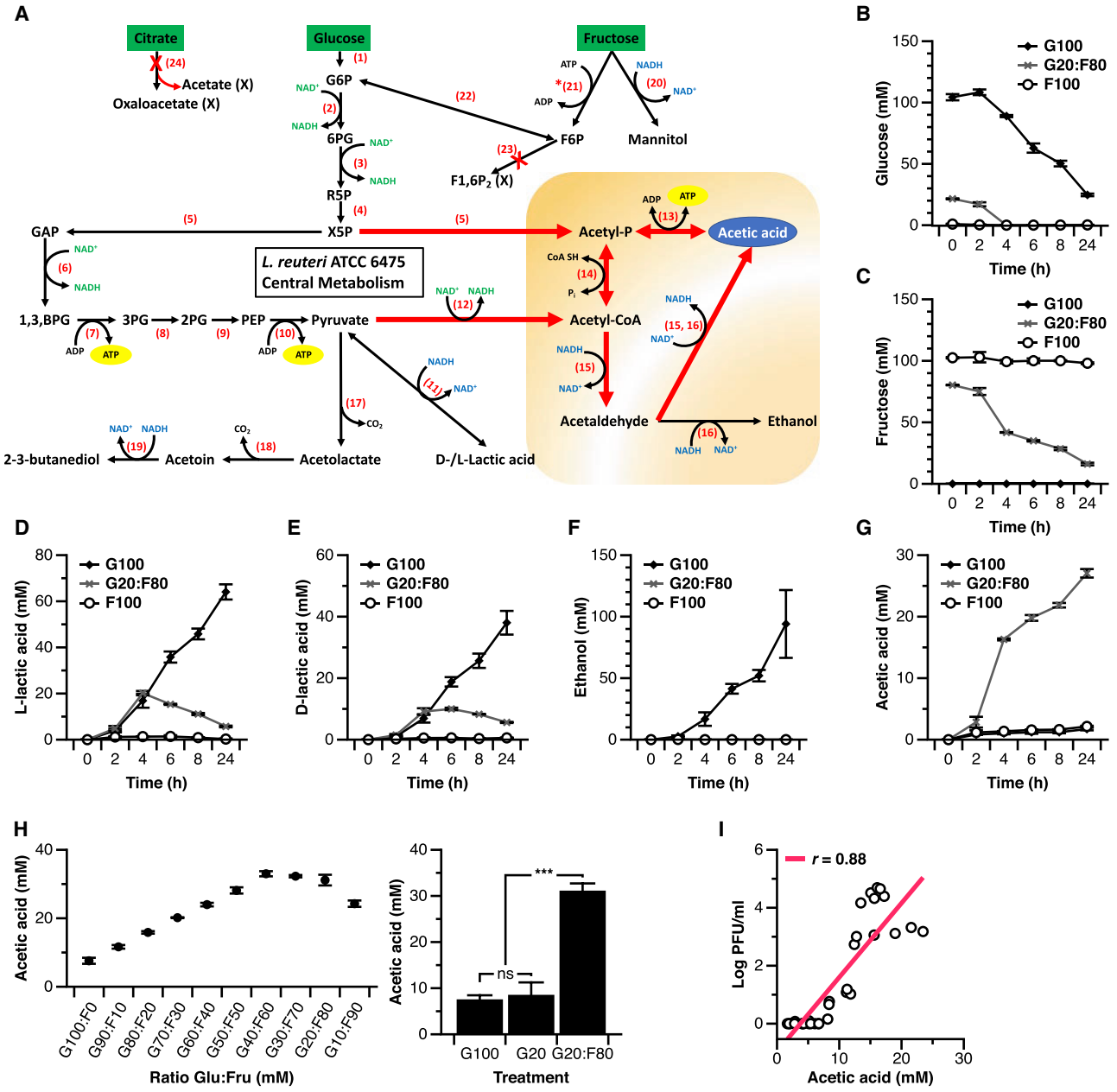

Figure 3. Central Metabolism of *L. reuteri* 6475 Is Linked to Phage Production

(A) Predicted central carbon metabolism in *L. reuteri* 6475 based on the genome sequence. Red arrows indicate prospective pathways by which acetic acid can be produced. Abbreviations of metabolic substrates and the predicted enzymes (numbers in parentheses) can be found in Table S2. Asterisk denotes pseudogene; X, absent.

(B–G) Characterization of metabolism and metabolic end products of *L. reuteri* during growth in mMRS containing different substrates. (B) consumption of glucose. (C) consumption of fructose. (D) production of L-lactic acid. (E) production of D-lactic acid. (F) production of ethanol. (G) production of acetic acid.

(H) Acetic acid production (mM) upon 24 hr growth of *L. reuteri* in mMRS containing 100 mM carbon source consisting of different ratios of glucose (G) and fructose (F). Right panel: acetic acid production in mMRS containing 100 mM glucose (G100), 20 mM glucose (G20), or a mixture of 20 mM glucose and 80 mM fructose (G20:F80). ns, no statistical significance ($p > 0.05$); ***$p < 0.001$. Data shown are means ± SD and are based on three biological replicates.

(I) Correlation between acetic acid production (mM) and phage production (log PFU/mL) as determined by the Pearson correlation coefficient (r). Data shown represent three biological replicates.

See also Figures S3 and S4; Table S2.

and 4E). Phage production was reduced by 500-fold in *L. reuteri ΔackA* when compared with the wild-type, and complementation of *ackA* restored phage production (Figure 4F). Not only do these findings indicate that *L. reuteri* 6475 has a pathway other than Ack by which cells produce acetic acid—possibly via the aforementioned bifunctional enzyme acetaldehyde

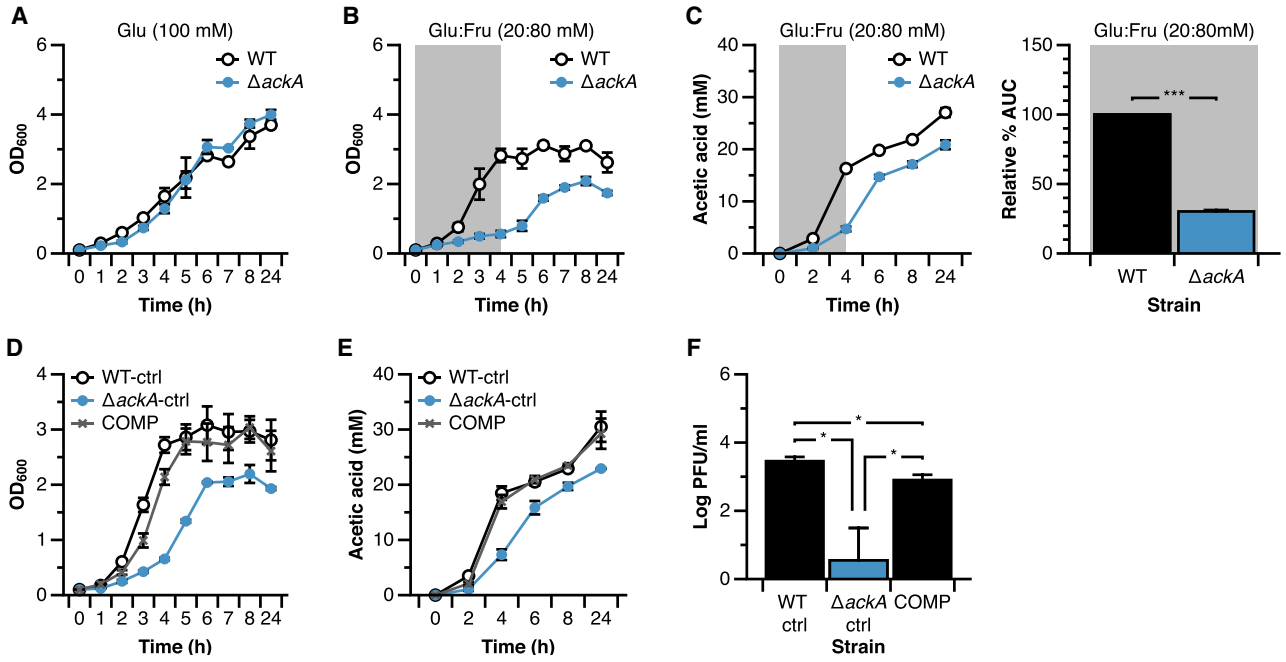

Figure 4. *L. reuteri* 6475 AckA Is Important for Acetic Acid and Phage Production

(A) Growth of *L. reuteri* wild-type (WT) and *L. reuteriΔackA* in mMRS containing 100 mM glucose.

(B) Growth of WT and *ΔackA* in mMRS containing 20 mM glucose and 80 mM fructose. Highlighted in gray is the period in which growth of *L. reuteriΔackA* is mostly delayed.

(C) Acetic acid production (mM) from WT and *ΔackA* in mMRS containing 20 mM glucose and 80 mM fructose. Right panel: area under the curve (AUC) of the acetic acid production by WT and *ΔackA* based on period 0–4 hr (highlighted in gray). ***$p < 0.001$.

(D–F) Growth (D), acetic acid production (mM) (E), and phage production (F) from *L. reuteri* WT harboring pSIP411 control plasmid (WT-ctrl), *L. reuteriΔackA* harboring pSIP411 (*ΔackA*-ctrl) and *L. reuteriΔackA* expressing AckA from plasmid pSIP (COMP). All cultured in mMRS harboring 20 mM glucose and 80 mM fructose. *$p < 0.05$.

Data shown are means ± SD and are based on three biological replicates.

dehydrogenase—it also strongly suggests that AckA drives acetic acid production during the early growth phases, as indicated by the highlighted regions in Figures 4B and 4C. Thus, these data suggest that the timing of acetic acid production by *L. reuteri* 6475 is of relevance to the production of phage.

Dietary Fructose Increases Intestinal Acetic Acid and *L. reuteri* 6475 Phage Production in AckA-Dependent Manner

To better understand the interplay between fructose metabolism, AckA, and phage production in the gut, we compared *L. reuteri* wild-type and *L. reuteriΔackA* in a diet crossover study in mice that received either glucose or fructose in their drinking water using the experimental design described above (Figure 2E). Compared with glucose, dietary fructose increased fecal acetic acid levels in animals that received *L. reuteri* wild-type (57.85_{Fru} versus 43.20_{Glu} mmol/kg; $p < 0.0001$), whereas fecal acetic levels between the fructose and glucose groups were not different when animals were administered *L. reuteriΔackA* (49.39_{Fru} versus 46.52_{Glu} mmol/kg; $p = 0.29$) (Figure 5A). Dietary fructose also resulted in 1.5-fold more phage in the fecal material when compared with dietary glucose ($1.5 \times 10^4_{GLU}$ versus $2.2 \times 10^4_{FRU}$ PFU/100 mg feces; $p < 0.0001$) when animals received *L. reuteri* wild-type (Figure 5B). In contrast, in animals fed *L. reuteriΔackA* and fructose, we recovered fewer phages compared with the glucose group ($6.2 \times 10^4_{GLU}$ versus $4.2 \times 10^4_{FRU}$ PFU/100 mg feces; $p = 0.0025$; Figure 5B), although the number of recovered bacteria was similar between treatment groups ($p > 0.2$; Figure 5C). These findings indicate that the Ack pathway contributes to both acetic acid production of *L. reuteri* and the induction of prophages in the gut of mice in response to dietary fructose.

Short-Chain Fatty Acids Promote Phage Production in *L. reuteri*

Next, we addressed whether acetic acid exposure, rather than metabolism, can trigger phage production by *L. reuteri*. This question is of relevance because in the colon, the dominant SCFA is acetic acid. Depending on the diet, and the location in the colon, the total concentration of SCFAs can be as high as 150 mmol/L (den Besten et al., 2013), with acetic acid, propionic acid, and butyric acid being present at a ratio of 60:20:20 (Koh et al., 2016). When we supplemented the growth medium with 100 mM acetic acid and adjusted the pH to 6.5, we recovered 1,000-fold more phage compared with the medium control lacking acetic acid (Figure 6A). The other main SCFAs, butyric acid and propionic acid, also promoted phage production, while lactic acid did not affect phage release. None of the SCFAs suppressed growth at the concentrations tested; in fact, subtle but significant increases in the final cell density were recorded

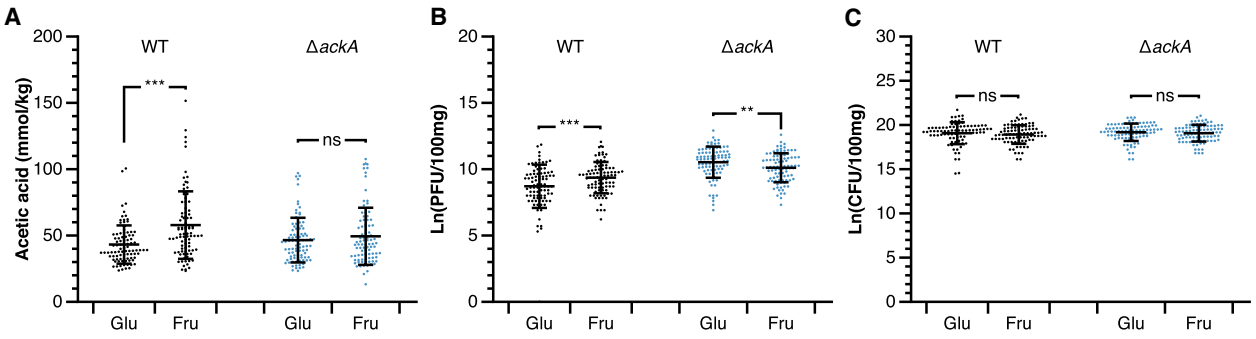

Figure 5. Dietary Fructose Combined with *L. reuteri* 6475 Administration Increases Intestinal Acetic Acid and Phage Production in an AckA-Dependent Manner

(A–C) Acetic acid concentration (A), phage numbers (B), and cell numbers (C) of *L. reuteri* in fecal samples obtained of mice receiving in their drinking water glucose (Glu) or fructose (Fru) in a crossover design and an administration of either *L. reuteri* 6475 wild-type (WT) or *L. reuteri ΔackA* (*ΔackA*). See STAR Methods for experimental details. Each dot represents a single data point from a single mouse on one day. Mice were sampled daily when administered *L. reuteri* and sugar water. The horizontal bars represent means and SD. CFU and PFU data are expressed as the natural log (ln). Data were analyzed with the linear mixed-effects model with repeated measures. Each dot represents a single data point from a single mouse; the horizontal bars represent means and SD. ns, no statistical significance ($p > 0.05$); **$p < 0.01$; ***$p < 0.001$.

when *L. reuteri* was supplemented with SCFAs (Figure 6A). Thus, all three major SCFAs trigger phage production by *L. reuteri* independent of pH. To analyze the SCFA dose dependency on phage induction, we exposed *L. reuteri* to 10–60 mM acetic acid, and recorded a positive correlation between acetic acid exposure and phage production (Figures 6B and 6C; Pearson's $r = 0.91$, $p < 0.001$). Thus, intestinal SCFAs are strong stimuli of prophage induction in *L. reuteri*. When we assessed the distribution of phages upon growth in media containing acetic acid or the SCFA mixture, we observed that both phages were produced, whereas growth in 20:80 mM glucose/fructose predominantly produced LRΦ1 (Figure S5), and warrant a separate study to investigate the dynamics of phage production in different environments.

SCFAs Induce Phage Production by Activation of the Ack Pathway

Next, we aimed to understand by which mechanism SCFAs promote *L. reuteri* phage production. Recently, it was shown in *Campylobacter jejuni* that SCFAs activate the Pta-Ack pathway (Luethy et al., 2017), which is important for efficient colonization of the chicken GI tract (Hendrixson and DiRita, 2004). To test whether SCFAs promote *L. reuteri* acetic acid production, and thus phage production, we supplemented MRS with the different SCFAs (acetic acid, propionic acid, and butyric acid), after we adjusted the pH to 6.5, and measured after 24 hr the net gain in acetic acid production. At different levels each individual SCFA, and the mixture, promoted acetic acid production in *L. reuteri* compared with the medium control lacking SCFAs (Figure 6D). To assess whether SCFAs promote acetic acid production via the Ack pathway, we supplemented the growth media of *L. reuteri ΔackA* with the different SCFAs. All SCFAs yielded less acetic acid production compared with the wild-type, although the differences that were observed between wild-type and *ΔackA* following growth in the presence of butyric acid were small (Figure 6D). However, supplementation of each SCFA, or mixture, yielded approximately 100-fold fewer phages in the *ΔackA* background compared with the wild-type (Figure 6E). Thus, SCFAs promote phage production in *L. reuteri* 6475 via the Ack pathway.

Phage Production in *L. reuteri* 6475 Is RecA Dependent

So far, we have identified fructose and SCFAs as triggers that promote phage production in *L. reuteri* 6475, but questions remain about the underlying mechanism by which prophages are induced. Many prophages have hijacked the SOS response, a pathway that is mostly known for its role in bacterial DNA damage response (reviewed in Kreuzer, 2013). Activation of the SOS response results in the activation of prophages. A key protein responsible for activation of the SOS response is RecA, which—at least in *Escherichia coli*—governs autocleavage of a prophage repressor that subsequently leads to prophage excision, replication, and cell lysis (Little, 1984). To understand whether acetic acid induces the SOS response, we inactivated *recA* (*L. reuteri ΔrecA*), thereby disarming the SOS system. Compared with the wild-type, *L. reuteri ΔrecA* had a reduced growth rate (Figure S6), which is in line with observations made in *L. lactis* (Duwat et al., 1995), a model organism of lactic acid bacteria. Inactivation of *recA* completely abolished phage induction following mitomycin C treatment, growth in 20:80 mM glucose/fructose, or a mixture of SCFAs (Figure 7A). Thus, dietary fructose and SCFAs induce phage production in *L. reuteri* 6475 in a RecA-dependent manner.

Fructose and SCFAs Promote Phage Production in Other Lactic Acid Bacteria

To test whether these triggers are unique for *L. reuteri* 6475, we also tested *L. reuteri* ATCC 55730—a strain that putatively encodes three complete prophages—and *Lactococcus lactis* NZ9000, which is lysogenized with ΦTP901 (Stockdale et al., 2013). Fructose increased phage production only in *L. reuteri* ATCC 55730, while acetic acid or a 60:20:20 mM mix of acetic/butyric/propionic acids increased phage production in both strains (Figures 7B and 7C), which implies that our findings are not specific to *L. reuteri* 6475 and could constitute a broader mechanism by which prophages are induced in the GI tract.

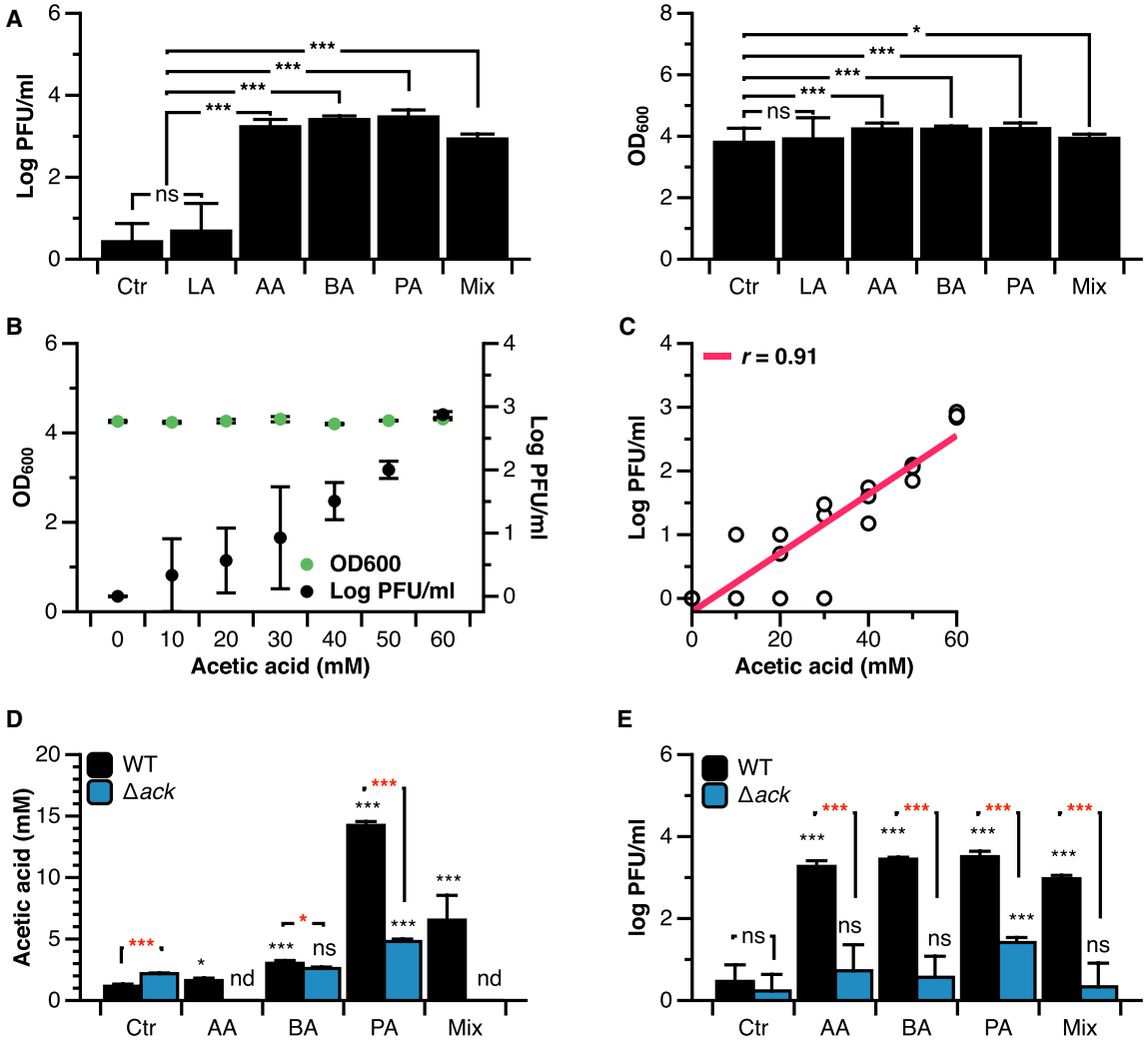

Figure 6. Short-Chain Fatty Acids Promote *L. reuteri* 6475 Phage Production in an AckA-Dependent Manner

(A) Phage production of *L. reuteri* following 24 hr growth in mMRS (ctrl), mMRS containing 100 mM lactic acid (LA), acetic acid (AA), butyric acid (BA), propionic acid (PA), or a 60:20:20 mixture of AA/PA/BA. Right panel: cell densities following growth in mMRS supplemented with different SCFAs. Data shown are means ± SD and are based on three biological replicates. ns, no statistical significance ($p > 0.05$); *$p < 0.05$; ***$p < 0.001$.

(B) Optical densities of *L. reuteri* cultures (green; primary y axis) and phage production (black; secondary y axis) upon 24 hr growth in mMRS (0) or in mMRS containing 10–60 mM acetic acid. Data shown are means ± SD and are based on three biological replicates.

(C) Correlation between acetic acid concentrations (mM) and phage production (log PFU/mL) as determined by the Pearson correlation coefficient (r).

(D and E) Acetic acid production (D), and phage production (E) from *L. reuteri* wild-type (WT, black bars) or *L. reuteri ΔackA* (*Δack*, blue bars) upon 24 hr growth in mMRS (ctrl) or mMRS containing SCFAs. Data shown are means ± SD and are based on three independent experiments. Black asterisks above the black and blue bars indicate statistical significance compared with the WT control and *ΔackA* control, respectively. Red asterisks indicate statistical significance between WT and *ΔackA* within the same condition. nd. not detected; ns. no statistical significance ($p > 0.05$); *$p < 0.05$; ***$p < 0.001$.

See also Figure S5.

DISCUSSION

In this study, we aimed to unravel diet-related cues that contribute to *L. reuteri* lysogenic induction and phage production in the GI tract. We discovered that dietary fructose, or exposure to the most abundant SCFAs found in the colon, activated the Ack pathway of *L. reuteri*, which in turn promoted phage production in a RecA-dependent manner.

Activation of the Ack pathway by SCFAs has recently been established in *C. jejuni* (Luethy et al., 2017). It was proposed that activation of this pathway is an advantage to the organism because it provides the cells with additional ATP, and thus more energy for growth in the gut. Also in *L. reuteri*, exposure to SCFAs activates the Ack pathway and phage production. However, inactivation of *ackA* did not completely shut down production of acetic acid and phage upon exposure to propionic acid. This suggests that propionic acid promotes the production of acetic acid and phage partly independent of AckA, possibly via the NAD^+-dependent acetaldehyde dehydrogenase pathway. That the Ack pathway is not the sole driver of phage production is also evident from our *in vivo* data, as *L. reuteri ΔackA* still produced phage during *in vivo* transit. In

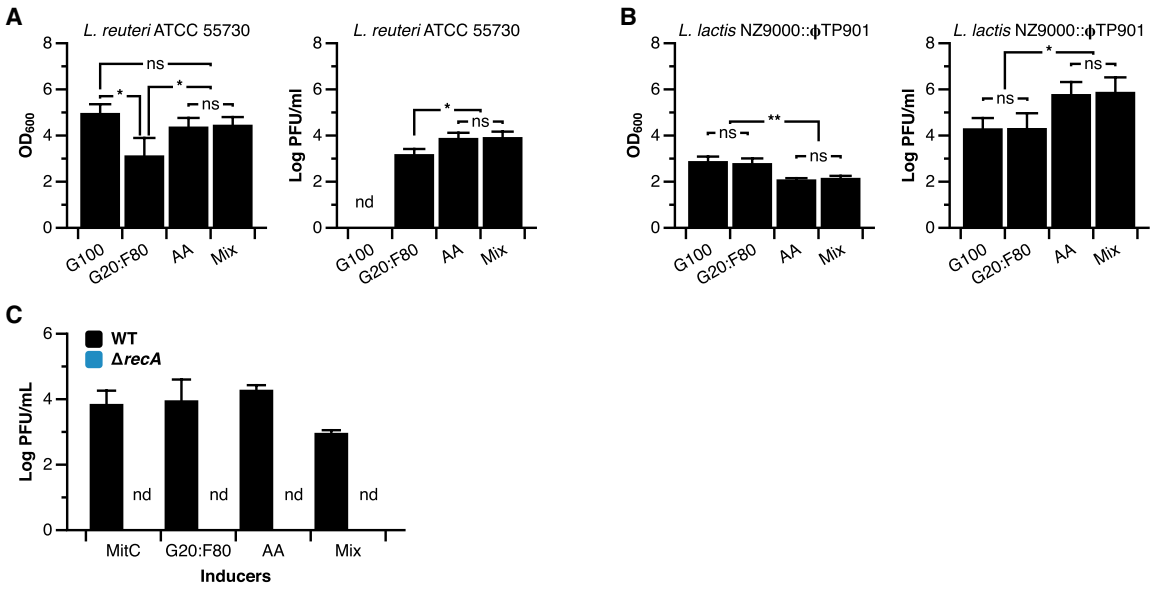

Figure 7. Fructose and SCFAs Promote Phage Production in Other Lactic Acid Bacteria, which in *L. reuteri* 6475 Is Driven in a RecA-Dependent Manner

(A) *L. reuteri* 6475 wild-type (WT) or *L. reuteri* 6475Δ*recA* (Δ*recA*) were challenged with mitomycin C, or cultured 24 hr in mMRS containing 20 mM glucose and 80 mM fructose (G20:F80), mMRS containing 100 mM glucose and 100 mM acetic acid (AA), or mMRS containing 100 mM glucose and 100 mM SCFA-mix: 60:20:20 mM acetic/propionic/butyric acids (Mix).

(B) Optical density of *L. reuteri* ATCC 55730 cultured 24 hr mMRS containing 100 mM glucose (G100), 20 mM glucose and 80 mM fructose (G20:F80), 100 mM acetic acid (AA), or a 60:20:20 mM mix of acetic/butyric/propionic acids (Mix). Right panel: phage production by *L. reuteri* ATCC 55730.

(C) Optical density of *L. lactis* NZ9000::ΦTP901 cultured 24 hr in mM17 containing 100 mM glucose (G100), 20 mM glucose and 80 mM fructose (G20:F80), 100 mM acetic acid (AA), or a 60:20:20 mM mix of acetic/butyric/propionic acids. Right panel: phage production by *L. lactis* NZ9000::ΦTP901.

All data represent means ± SD and are based on three biological replicates. ns, no statistical significance ($p > 0.05$); nd, not detected; *$p < 0.05$; **$p < 0.01$. See also Figure S6.

fact, we observed higher phage production when animals were supplemented with glucose and *L. reuteri*Δ*ackA* compared with the wild-type. Possibly, the intestinal environment changes the metabolic flux in *L. reuteri* partly toward the Ack pathway. Subsequent inactivation of *ackA* could lead to increased accumulation of toxic intermediates, such as acetaldehyde. Acetaldehyde is a known DNA-damaging agent (Dellarco, 1988), which is likely to lead to activation of RecA and subsequent prophage induction. However, this remains speculative as it is currently not possible to measure the metabolic flux of *L. reuteri* during GI transit.

L. reuteri can reduce fructose to mannitol (Arsköld et al., 2008; Rodriguez et al., 2012). The microbiota, at least in pigs, can convert mannitol to SCFAs (Maekawa et al., 2005). However, our data show that the increase in acetic acid from mice fed fructose and *L. reuteri* is driven by *L. reuteri* AckA. This suggests that conversion of mannitol by the mouse microbiota is not a major source of acetic acid production. This was previously shown in rats, where dietary supplementation of mannitol did not increase acetic and propionic acids, which means that the microbiota in different hosts have different potential to convert mannitol to SCFAs (Maekawa et al., 2005). Thus, the combination of environmental SCFAs and activation of the Ack pathway via fructose metabolism is one mechanism by which *L. reuteri* modulates phage production in the gut.

In vitro fructose metabolism increased phage production by up to 10,000-fold. *In vivo*, differences in phage production between the two arms were consistent before and after the washout period: fructose supplementation yielded a relatively small, but highly significant, increase in phage production compared with the glucose group. There are a couple of reasons why the magnitude of phage production *in vivo* was much lower than that observed *in vitro*. First, the gut is a complex ecosystem and multiple factors are likely to contribute to *L. reuteri* phage production, which may mask the additive effects of dietary fructose. Second, lactobacilli are generally fastidious organisms that mostly use simple sugars for growth (Walter, 2008). While sugars like fructose and trehalose can reach the lower intestine (Collins et al., 2018; Jang et al., 2018), the general availability of simple sugars is scarce in the colon where anaerobic bacteria mostly ferment non-digestible fibers (Wong et al., 2006). We showed that low availability of glucose is a driver of phage production in *L. reuteri*, which suggests that nutrient starvation in the colon could contribute to phage production. Finally, as clearly shown in our study, environmental SCFAs are a major inducer of phage production. These factors collectively contribute to the rather high "basal" levels of *L. reuteri* phages in the gut (Figure 1), which are likely to mask the effect of fructose on *L. reuteri* phage production—especially when taking into consideration that *L. reuteri* has to compete with other members of the microbiota for available fructose. Nonetheless, dietary supplementation of fructose did increase phage production, which we demonstrated was dependent on AckA.

So, why are phages produced upon activation of the Ack pathway? At this point, we can only speculate that this is linked to activation of the SOS response. Future experiments should focus on an elucidation of the underlying mechanisms by which the activation of the acetogenesis pathway is linked to induction of the SOS response. We are in the process of testing the hypothesis that acetic acid production activates the SOS response due to a reduction in the intracellular pH (pH_i). At least in *E. coli*, changes in pH_i damages DNA and activates the SOS response (Schuldiner et al., 1986), and similar mechanisms might underlie prophage induction in *L. reuteri*.

In summary, we have unraveled one of the underlying mechanisms by which a lysogenic strain of the gut symbiont *L. reuteri* produces phage in the gut, how this affects the bacterial host, and how this is related to dietary substrates and metabolic end products affected by diet. Our findings provide a potential mechanistic explanation for the pronounced impact of dietary changes on the phageome, and potentially even bacteriome communities. For example, Minot et al. (2011) showed that the phageome community diverged to a new state that was driven by a diet low in fat and enriched in fiber. Individuals consuming a high-fiber diet will most likely have increased SCFAs in the gut (reviewed in Ríos-Covián et al., 2016), which our study identified as one of the drivers of phage production, and could explain changes in the phageome community. Our results are also interesting in light of the findings by Howe et al. (2016), who demonstrated that a diet enriched in sucrose, a disaccharide of glucose and fructose, increases the abundance of virus-like particles. Most importantly, their metagenome analyses revealed several contigs with homology to *L. reuteri* phages in response to the high-sugar diet. The work by Howe et al. (2016), combined with our findings, also have broader implications as they suggest that a diet patterns (high sugar) that resemble the Western diet induce prophages that can affect bacterial populations, potentially by two mechanisms. First, the bacterial community may be altered following prophage induction, as this leads to lysis of the lysogen. Second, the released prophages may have a profound effect on the bacterial community structure as they can kill closely related species, as was previously was demonstrated for *Enterococcus faecalis*: phage-producing *E. faecalis* outcompeted other *E. faecalis* strains in the gut (Duerkop et al., 2012). Collectively, these could provide a yet unexplored mechanism for the decline in microbiota diversity through industrialization (Deehan and Walter, 2016). Clearly, further studies are needed to investigate the role of diet and other factors that affect gut microbiomes, as well as prophage induction and its implications on gut microbial ecology. Our study provides a proof of concept that such an understanding can be achieved by the application of a genetic approach to develop a gut symbiont as a model system to study its prophages. If applied in the right ecological context, such an approach paves the way to initiating studies to help us understand the ecological role of gut phages. This, combined with mechanistic understanding of diet-induced phage production, would provide a basic understanding to tailor the robustness of select organisms in the gut, including probiotics, and develop improved strategies to modulate gut microbial communities and improve animal and human health.

STAR★METHODS

Detailed methods are provided in the online version of this paper and include the following:

- KEY RESOURCES TABLE
- CONTACT FOR REAGENT AND RESOURCE SHARING
- EXPERIMENTAL MODEL AND SUBJECT DETAILS
  - Bacterial Strains and Growth Conditions
  - Growth Rate
  - Mice
- METHOD DETAILS
  - Reagents and Enzymes
  - Mitomycin C Induction
  - Identification of Prophages in *L. reuteri* 6475
  - Identification of Prophage Excision and *attB* Sites in *L. reuteri* 6475
  - Phage Production in Media with Different Carbohydrates
  - Construction of Prophage Deletion Strains
  - Plaque Assay for *L. reuteri* 6475 Phages
  - Construction of Rifampicin-Resistant Derivatives and Inactivation of *ackA*, *recA*, and *mdh*
  - Complementation of *ackA*
  - *In Silico* Analysis to Map the Central Metabolism in *L. reuteri* 6475
  - Metabolic End-Product Analysis
  - *L. reuteri* Survival and Phage Production during GI Transit in Mice
  - Two-Arm Dietary Crossover Study
- QUANTIFICATION AND STATISTICAL ANALYSIS
  - Statistics
- DATA AND SOFTWARE AVAILABILITY

SUPPLEMENTAL INFORMATION

Supplemental Information includes six figures and two tables and can be found with this article online at https://doi.org/10.1016/j.chom.2018.11.016.

ACKNOWLEDGMENTS

We thank D. van Sinderen for comments. We are grateful to the College of Agricultural Life Sciences Statistical Consulting Lab for their assistance in the statistical analysis. We thank Stefan Roos (BioGaia, Stockholm, Sweden) for providing *L. reuteri* ATCC PTA 6475 and *L. reuteri* ATCC 55730. We thank O'Reilly Science Art for assistance with preparing the graphical abstract. J.P.v.P. thanks the University of Wisconsin-Madison Food Research Institute (233-PRJ75PW) and BioGaia (Stockholm, Sweden; 233-AAB1492) for financial support. Finally, we thank the anonymous reviewers for their constructive feedback, which collectively improved our manuscript.

AUTHOR CONTRIBUTIONS

J.-H.O. designed and performed the experiments, analyzed and interpreted the data, and wrote and revised the manuscript; L.M.A. performed experiments, provided technical support, and revised the manuscript; M.P. provided technical support; K.L.S., M.P.K., and A.D.A. provided technical support and shared resources; J.W. contributed to data interpretation and wrote and revised the manuscript; J.P.v.P. secured funding, conceived, designed, and supervised the study, and wrote and critically revised the manuscript.

DECLARATION OF INTERESTS

J.P.v.P. received unrestricted funds from BioGaia. The other authors declare no competing interests.

Received: June 21, 2018
Revised: September 10, 2018
Accepted: November 28, 2018
Published: January 15, 2019

REFERENCES

Alonso, R., Mateo, E., Churruca, E., Martinez, I., Girbau, C., and Fernández-Astorga, A. (2005). MAMA-PCR assay for the detection of point mutations associated with high-level erythromycin resistance in *Campylobacter jejuni* and *Campylobacter coli* strains. J. Microbiol. Methods *63*, 99–103.

Arndt, D., Grant, J.R., Marcu, A., Sajed, T., Pon, A., Liang, Y., and Wishart, D.S. (2016). PHASTER: a better, faster version of the PHAST phage search tool. Nucleic Acids Res. *44*, W16–W21.

Arsköld, E., Lohmeier-Vogel, E., Cao, R., Roos, S., Rådström, P., and van Niel, E.W.J. (2008). Phosphoketolase pathway dominates in *Lactobacillus reuteri* ATCC 55730 containing dual pathways for glycolysis. J. Bacteriol. *190*, 206–212.

den Besten, G., van Eunen, K., Groen, A.K., Venema, K., Reijngoud, D.-J., and Bakker, B.M. (2013). The role of short-chain fatty acids in the interplay between diet, gut microbiota, and host energy metabolism. J. Lipid Res. *54*, 2325–2340.

Breitbart, M., Hewson, I., Felts, B., Mahaffy, J.M., Nulton, J., Salamon, P., and Rohwer, F. (2003). Metagenomic analyses of an uncultured viral community from human feces. J. Bacteriol. *185*, 6220–6223.

Canchaya, C., Proux, C., Fournous, G., Bruttin, A., and Brüssow, H. (2003). Prophage genomics. Microbiol. Mol. Biol. Rev. *67*, 238–276.

Christiansen, B., Johnsen, M., Stenby, E., Vogensen, F., and Hammer, K. (1994). Characterization of the lactococcal temperate phage TP901-1 and its site-specific integration. J. Bacteriol. *176*, 1069–1076.

Collins, J., Robinson, C., Danhof, H., Knetsch, C.W., van Leeuwen, H.C., Lawley, T.D., Auchtung, J.M., and Britton, R.A. (2018). Dietary trehalose enhances virulence of epidemic *Clostridium difficile*. Nature *553*, 291–294.

Cornuault, J.K., Petit, M.A., Mariadassou, M., Benevides, L., Moncaut, E., Langella, P., Sokol, H., and De Paepe, M. (2018). Phages infecting *Faecalibacterium prausnitzii* belong to novel viral genera that help to decipher intestinal viromes. Microbiome *6*, 65.

David, L.A., Maurice, C.F., Carmody, R.N., Gootenberg, D.B., Button, J.E., Wolfe, B.E., Ling, A.V., Devlin, A.S., Varma, Y., Fischbach, M.A., et al. (2013). Diet rapidly and reproducibly alters the human gut microbiome. Nature *505*, 559–563.

Deehan, E.C., and Walter, J. (2016). The fiber gap and the disappearing gut microbiome: implications for human nutrition. Trends Endocrinol. Metab. *27*, 239–242.

Dellarco, V.L. (1988). A mutagenicity assessment of acetaldehyde. Mutat. Res. *195*, 1–20.

Diard, M., Bakkeren, E., Cornuault, J.K., Moor, K., Hausmann, A., Sellin, M.E., Loverdo, C., Aertsen, A., Ackermann, M., De Paepe, M., et al. (2017). Inflammation boosts bacteriophage transfer between *Salmonella* spp. Science *355*, 1211–1215.

Duar, R.M., Lin, X.B., Zheng, J., Martino, M.E., Grenier, T., Perez-Munoz, M.E., Leulier, F., Ganzle, M., and Walter, J. (2017). Lifestyles in transition: evolution and natural history of the genus *Lactobacillus*. FEMS Microbiol. Rev. *41* (Supp_1), S27–S48.

Duerkop, B.A., Clements, C.V., Rollins, D., Rodrigues, J.L.M., and Hooper, L.V. (2012). A composite bacteriophage alters colonization by an intestinal commensal bacterium. Proc. Natl. Acad. Sci. U S A *109*, 17621–17626.

Duerkop, B.A., Kleiner, M., Paez-Espino, D., Zhu, W., Bushnell, B., Hassell, B., Winter, S.E., Kyrpides, N.C., and Hooper, L.V. (2018). Murine colitis reveals a disease-associated bacteriophage community. Nat. Microbiol. *3*, 1023–1031.

Duwat, P., Ehrlich, S.D., and Gruss, A. (1995). The recA gene of *Lactococcus lactis*: characterization and involvement in oxidative and thermal stress. Mol. Microbiol. *17*, 1121–1131.

Hatfull, G.F. (2008). Bacteriophage genomics. Curr. Opin. Microbiol. *11*, 447–453.

Hendrixson, D.R., and DiRita, V.J. (2004). Identification of *Campylobacter jejuni* genes involved in commensal colonization of the chick gastrointestinal tract. Mol. Microbiol. *52*, 471–484.

Howe, A., Ringus, D.L., Williams, R.J., Choo, Z.N., Greenwald, S.M., Owens, S.M., Coleman, M.L., Meyer, F., and Chang, E.B. (2016). Divergent responses of viral and bacterial communities in the gut microbiome to dietary disturbances in mice. ISME J. *10*, 1217–1227.

Jang, C., Hui, S., Lu, W., Cowan, A.J., Morscher, R.J., Lee, G., Liu, W., Tesz, G.J., Birnbaum, M.J., and Rabinowitz, J.D. (2018). The small intestine converts dietary fructose into glucose and organic acids. Cell Metab. *27*, 351–361.e3.

Johnson, R.J., Segal, M.S., Sautin, Y., Nakagawa, T., Feig, D.I., Kang, D.H., Gersch, M.S., Benner, S., and Sanchez-Lozada, L.G. (2007). Potential role of sugar (fructose) in the epidemic of hypertension, obesity and the metabolic syndrome, diabetes, kidney disease, and cardiovascular disease. Am. J. Clin. Nutr. *86*, 899–906.

Kandler, O., Stetter, K.-O., and Köhl, R. (1980). *Lactobacillus reuteri* sp. nov., a new species of heterofermentative lactobacilli. Zentralbl. Bakteriol. Hyg. Abt. I Orig. C *1*, 264–269.

Kleiner, M., Hooper, L.V., and Duerkop, B.A. (2015). Evaluation of methods to purify virus-like particles for metagenomic sequencing of intestinal viromes. BMC Genomics *16*, 7.

Koh, A., De Vadder, F., Kovatcheva-Datchary, P., and Bäckhed, F. (2016). From dietary fiber to host physiology: short-chain fatty acids as key bacterial metabolites. Cell *165*, 1332–1345.

de Kok, S., Stanton, L.H., Slaby, T., Durot, M., Holmes, V.F., Patel, K.G., Platt, D., Shapland, E.B., Serber, Z., and Dean, J. (2014). Rapid and reliable DNA assembly via ligase cycling reaction. ACS Synth. Biol. *3*, 97–106.

Kreuzer, K.N. (2013). DNA damage responses in prokaryotes: regulating gene expression, modulating growth patterns, and manipulating replication forks. Cold Spring Harb. Perspect. Biol. *5*, a012674.

Leenhouts, K., Bolhuis, A., Venema, G., and Kok, J. (1998). Construction of a food-grade multiple-copy integration system for Lactococcus lactis. Appl. Microbiol. Biotechnol. *49*, 417–423.

Ley, R.E., Hamady, M., Lozupone, C., Turnbaugh, P.J., Ramey, R.R., Bircher, J.S., Schlegel, M.L., Tucker, T.A., Schrenzel, M.D., Knight, R., and Gordon, J.I. (2008). Evolution of mammals and their gut microbes. Science *320*, 1647–1651.

Little, J.W. (1984). Autodigestion of lexA and phage lambda repressors. Proc. Natl. Acad. Sci. U S A *81*, 1375–1379.

Luethy, P.M., Huynh, S., Ribardo, D.A., Winter, S.E., Parker, C.T., and Hendrixson, D.R. (2017). Microbiota-derived short-chain fatty acids modulate expression of *Campylobacter jejuni* determinants required for commensalism and virulence. mBio *8*, e00407–00417.

Maekawa, M., Maekawa, M., Ushida, K., Hoshi, S., Kashima, N., Ajisaka, K., Maekawa, M., Ushida, K., Hoshi, S., Kashima, N., et al. (2005). Butyrate and propionate production from D-mannitol in the large intestine of pig and rat. Microb. Ecol. Health Dis. *17*, 169–176.

Manrique, P., Bolduc, B., Walk, S.T., van der Oost, J., de Vos, W.M., and Young, M.J. (2016). Healthy human gut phageome. Proc. Natl. Acad. Sci. U S A *113*, 10400–10405.

Martínez, I., Kim, J., Duffy, P.R., Schlegel, V.L., and Walter, J. (2010). Resistant starches types 2 and 4 have differential effects on the composition of the fecal microbiota in human subjects. PLoS One *5*, e15046.

Milliken, G.A., and Johnson, D.E. (2001). Analysis of Messy Data, Volume III: Analysis of Covariance (Chapman and Hall/CRC).

Minot, S., Sinha, R., Chen, J., Li, H., Keilbaugh, S.A., Wu, G.D., Lewis, J.D., and Bushman, F.D. (2011). The human gut virome: inter-individual variation and dynamic response to diet. Genome Res. *21*, 1616–1625.

Natividad, J.M., Agus, A., Planchais, J., Lamas, B., Jarry, A.C., Martin, R., Michel, M.L., Chong-Nguyen, C., Roussel, R., Straube, M., et al. (2018). Impaired aryl hydrocarbon receptor ligand production by the gut microbiota is a key factor in metabolic syndrome. Cell Metab. *28*, 737–749.e4.

Nilsson, A.G., Sundh, D., Backhed, F., and Lorentzon, M. (2018). *Lactobacillus reuteri* reduces bone loss in older women with low bone mineral density: a randomized, placebo-controlled, double-blind, clinical trial. J. Intern. Med. https://doi.org/10.1111/joim.12805.

Oh, J.-H., and van Pijkeren, J.-P. (2014). CRISPR-Cas9-assisted recombineering in *Lactobacillus reuteri*. Nucleic Acids Res. *42*, e131.

Oh, P.L., Benson, A.K., Peterson, D.A., Patil, P.B., Moriyama, E.N., Roos, S., and Walter, J. (2010). Diversification of the gut symbiont *Lactobacillus reuteri* as a result of host-driven evolution. ISME J. *4*, 377–387.

van Pijkeren, J.-P., and Britton, R.A. (2012). High efficiency recombineering in lactic acid bacteria. Nucleic Acids Res. *40*, e76.

Reyes, A., Semenkovich, N.P., Whiteson, K., Rohwer, F., and Gordon, J.I. (2012). Going viral: next-generation sequencing applied to phage populations in the human gut. Nat. Rev. Microbiol. *10*, 607–617.

Ríos-Covián, D., Ruas-Madiedo, P., Margolles, A., Gueimonde, M., de los Reyes-Gavilán, C.G., and Salazar, N. (2016). Intestinal short chain fatty acids and their link with diet and human health. Front. Microbiol. *7*, 185.

Rodriguez, C., Rimaux, T., Fornaguera, M.J., Vrancken, G., de Valdez, G.F., De Vuyst, L., and Mozzi, F. (2012). Mannitol production by heterofermentative *Lactobacillus reuteri* CRL 1101 and *Lactobacillus fermentum* CRL 573 in free and controlled pH batch fermentations. Appl. Microbiol. Biotechnol. *93*, 2519–2527.

Schuldiner, S., Agmon, V., Brandsma, J., Cohen, A., Friedman, E., and Padan, E. (1986). Induction of SOS functions by alkaline intracellular pH in *Escherichia coli*. J. Bacteriol. *168*, 936–939.

Sørvig, E., Grönqvist, S., Naterstad, K., Mathiesen, G., Eijsink, V.G., and Axelsson, L. (2003). Construction of vectors for inducible gene expression in Lactobacillus sakei and L. plantarum. FEMS Microbiol. Lett. *229*, 119–126.

Sørvig, E., Mathiesen, G., Naterstad, K., Eijsink, V.G.H., and Axelsson, L. (2005). High-level, inducible gene expression in *Lactobacillus sakei* and *Lactobacillus plantarum* using versatile expression vectors. Microbiology *151* (Pt 7), 2439–2449.

Stockdale, S.R., Mahony, J., Courtin, P., Chapot-Chartier, M.-P., van Pijkeren, J.-P., Britton, R.A., Neve, H., Heller, K.J., Aideh, B., Vogensen, F.K., and van Sinderen, D. (2013). The lactococcal phages Tuc2009 and TP901-1 incorporate two alternate forms of their tail fiber into their virions for infection specialization. J. Biol. Chem. *288*, 5581–5590.

Vos, M.B., Kimmons, J.E., Gillespie, C., Welsh, J., and Blanck, H.M. (2008). Dietary fructose consumption among US children and adults: the third national health and nutrition examination survey. Medscape J. Med. *10*, 160.

Walter, J. (2008). Ecological role of lactobacilli in the gastrointestinal tract: implications for fundamental and biomedical research. Appl. Environ. Microbiol. *74*, 4985–4996.

Walter, J., Britton, R.A., and Roos, S. (2011). Host-microbial symbiosis in the vertebrate gastrointestinal tract and the *Lactobacillus reuteri* paradigm. Proc. Natl. Acad. Sci. U S A *108*, 4645–4652.

Wong, J.M., de Souza, R., Kendall, C.W., Emam, A., and Jenkins, D.J. (2006). Colonic health: fermentation and short chain fatty acids. J. Clin. Gastroenterol. *40*, 235–243.

Yatsunenko, T., Rey, F.E., Manary, M.J., Trehan, I., Dominguez-Bello, M.G., Contreras, M., Magris, M., Hidalgo, G., Baldassano, R.N., Anokhin, A.P., et al. (2012). Human gut microbiome viewed across age and geography. Nature *486*, 222–227.

Zelante, T., Iannitti, R.G., Cunha, C., De Luca, A., Giovannini, G., Pieraccini, G., Zecchi, R., D'Angelo, C., Massi-Benedetti, C., Fallarino, F., et al. (2013). Tryptophan catabolites from microbiota engage aryl hydrocarbon receptor and balance mucosal reactivity via interleukin-22. Immunity *39*, 372–385.

Zhang, S., Oh, J.H., Alexander, L.M., Ozcam, M., and van Pijkeren, J.P. (2018). d-Alanyl-d-alanine ligase as a broad-host-range counterselection marker in vancomycin-resistant lactic acid bacteria. J. Bacteriol. *200*, https://doi.org/10.1128/JB.00607-17.

Zheng, J., Ruan, L., Sun, M., and Gänzle, M. (2015). A genomic view of lactobacilli and pediococci demonstrates that phylogeny matches ecology and physiology. Appl. Environ. Microbiol. *81*, 7233–7243.

STAR★METHODS

KEY RESOURCES TABLE

REAGENT or RESOURCE	SOURCE	IDENTIFIER
Bacterial and Virus Strains		
Escherichia coli	Leenhouts et al., 1998, in *trans* RepA provider, Kan^R (*E. coli* cloning host)	EC1000
Escherichia coli	Zhang et al., 2018, EC1000 harboring pVPL3002, Em^R	VPL3002
Escherichia coli	This study, EC1000 harboring pVPL3590, Em^R	VPL3590
Escherichia coli	This study, EC1000 harboring pVPL3593, Em^R	VPL3593
Lactobacillus reuteri	Laboratory stock, 6475 harboring pJP042, Em^R	VPL3744
Escherichia coli	This study, EC1000 harboring pVPL3746, Em^R	VPL3746
Escherichia coli	This study, EC1000 harboring pVPL3749, Em^R	VPL3749
Escherichia coli	This study, EC1000 harboring pVPL3810, Em^R	VPL3810
Escherichia coli	This study, EC1000 harboring pVPL31093, Em^R	VPL31093
Lactococcus lactis ssp. *cremoris*	Stockdale et al., 2013, *Lactococcus lactis* harboring TP901-1 prophage	TP901-1
Lactococcus lactis ssp. *cremoris*	Christiansen et al., 1994, host strain for TP901-1 phage	3107
Lactococcus lactis ssp. *cremoris*	Laboratory stock, *Lactococcus lactis* MG1363 harboring pSIP411	VPL2005
Lactobacillus reuteri	BioGaia AB, this strain is also known as MM4-1A	ATCC PTA 6475
Lactobacillus reuteri	This study, VPL1014 ΔLRΦ1 Δ*attB1*	VPL4079
Lactobacillus reuteri	This study, VPL4079 ΔLRΦ1 Δ*attB1* ΔLRΦ2 Δ*attB2* (Lytic host for LRΦ1 and LRΦ2)	VPL4090 (LH)
Lactobacillus reuteri	This study, VPL1014 ΔLRΦ2 Δ*attB2*	VPL4104 (LRΦ2 LH)
Lactobacillus reuteri	This study, VPL4090::*attB2*	VPL4107
Lactobacillus reuteri	This study, VPL4107::*attB1*	VPL4121 (ΔΦ1ΔΦ2)
Lactobacillus reuteri	This study, VPL1014 *rpoB*::oVPL236 (T487S, H488R), Rif^R	VPL4126 (WT Rif^R)
Lactobacillus reuteri	This study, VPL4121 *rpoB*::oVPL236 (T487S, H488R), Rif^R	VPL4129 (ΔΦ1ΔΦ2 Rif^R)
Lactobacillus reuteri	This study, VPL1014 *recA*::oVPL2862 (V145X)	VPL4213 (Δ*recA*)
Lactobacillus reuteri	This study, VPL1014 *ackA*::oVPL2870 (H183X)	VPL4216 (Δ*ackA*)
Lactobacillus reuteri	This study, VPL4216 harboring pVPL31093	VPL31099 (*ackA*_COMP)
Lactobacillus reuteri	This study, VPL4216 harboring pSIP411	VPL31120
Lactobacillus reuteri	This study, VPL1014 *mdh*::oVPL3135 (P48X, G49X)	VPL4232 (Δ*mdh*)
Lactobacillus reuteri	Human isolate	ATCC 55730
Chemicals, Peptides, and Recombinant Proteins		
Agar	Alfa Aesar	Cat# A10752
Agarose	IBI	Cat# IB70042
LB broth	Acumedia, Neogen	Cat# 7290A
MRS broth	BD	Cat# 288110
M17 broth	BD	Cat# 218561
Potassium Buffered Saline	Gibco	Cat# 14190-144
Peptone	Fisher Scientific	Cat# BP9725-500
Beef extract	BD	Cat# 211520
Yeast extract	IBI	Cat# IB49160
Dipotassium phosphate	Fisher Scientific	Cat# P-290-500

(*Continued on next page*)

Continued

REAGENT or RESOURCE	SOURCE	IDENTIFIER
Ammonium citrate	Fluka	Cat# 09831
Magnesium sulfate	Fisher Scientific	Cat# M65-100LB
Manganese sulfate	SIGMA	Cat# M-7899
Tween 80	Sigma-Aldrich	Cat# RES3063T-A103X
Calcium chloride dihydrate	Fisher Scientific	Cat# C-79-500
Tris-HCl	Thermo Scientific	Cat# J22638-AP
L-Arabinose	Amresco	Cat# 1B1473
D-Fructose	SIGMA	Cat# F3510
D-Glucose	Sigma-Aldrich	Cat# G5767
D-Galactose	Dot Scientific	Cat# DSG33000
D-Maltose	Amresco	Cat# 1B1184
D-Xylose	Sigma-Aldrich	Cat# X1500-500G
D-/L-lactic acid	SIGMA	Cat# L1250-1L
Acetic acid	Sigma-Aldrich	Cat# 3863-50ML
Butyric acid	Fluka	Cat# 19210
Propionic acid	Fisher Scientific	Cat# A258-500
Chloramphenicol	Dot Scientific	Cat# DSC61000-25
Erythromycin	Fisher Scientific	Cat# BP920-25
Mitomycin C	SIGMA	Cat# M0503-5X2MG
Vancomycin	Chem-Impex	Cat# 00315
Ethanol	KOPTEC	Cat# V1016
P_{sak} Induction peptide	Peptide2.0	Sequence: MAGNSSNFIHKIKQIFTHR
Choice Taq DNA polymerase master mix	Denville Scientific	Cat# CB4070-8
Phusion Hot Start polymerase II	Thermo Scientific	Cat# F-549-L
T4 DNA ligase	Thermo Scientific	Cat# EL0011
Polynucleotide kinase	Thermo Scientific	Cat# EK0031
dATP	Promega	Cat# U120A
Ampligase	Lucigen	Cat# A32750
Sodium Hydroxide	Fisher Scientific	Cat# S318-500
HCl	Ricca Chemical Company	Cat# 3440-1
Critical Commercial Assays		
Qubit dsDNA quantification kit	Invitrogen	Cat# Q32853
GeneJET PCR purification kit	Thermo Scientific	Cat# K0701
Plasmid mini prep kit	Promega	Cat# A9340
Acetic acid assay kit	R-Biopharm AG	Cat# 10148261035
Glucose/Fructose assay kit	R-Biopharm AG	Cat# 10139106035
D-/L-Lactic acid assay kit	R-Biopharm AG	Cat# 11112821035
Ethanol assay kit	R-Biopharm AG	Cat# 10176290035
Deposited Data		
L. reuteri ATCC PTA 6475 LRΦ1 genome	GenBank: MH837542 (https://www.ncbi.nlm.nih.gov/genome/?term=MH837542)	
L. reuteri ATCC PTA 6475 LRΦ2 genome	GenBank: MH837543 (https://www.ncbi.nlm.nih.gov/genome/?term=MH837543)	
Experimental Models: Organisms/Strains		
C57BL/6J, Male	Jackson Laboratory	Cat# 000664
Oligonucleotides		
See Table S1 for primers used for this study		

(*Continued on next page*)

Continued

REAGENT or RESOURCE	SOURCE	IDENTIFIER
Software and Algorithms		
PHASTER	The Wishart Lab	http://phaster.ca/Datagrap
Pfam	EMBL-EBI	https://pfam.xfam.org/
KEGG	The Kanehisa Lab	https://www.genome.jp/kegg/
Image Lab	Bio-Rad	Ver. 6.0.1
SAS	SAS	Ver. 9.4
JMP Pro	SAS	Ver. 11.0.0
DataGraph	DataGraph	Ver. 4.2.1: https://www.visualdatatools.com
Other		
bMRS medium	1.0% peptone, 1.0% beef extract, 0.5% yeast extract, 0.2% dipotassium phosphate, 0.2% ammonium citrate, 0.01% magnesium sulfate, 0.005 % manganese sulfate (all w/v) and 0.1% (v/v) Tween 80, pH6.5	
mMRS medium	bMRS supplemented with carbon source(s) ± short-chain fatty acids	
pNZ8048::Em^R gene, Em^R	Lab stock, positive control for transformation efficiency	pVPL2042
pORI19::*ddlA* $F258Y_{reuteri}$, Em^R	Zhang et al., 2018, pORI19 derivative with *ddlA*F258Y counter-selection marker	pVPL3002
pVPL3002::*LRΦ1* deletion cassette, Em^R	This study, deletion cassette targets entire LRΦ1 and *attB1*	pVPL3590
pVPL3002::*LRΦ2* deletion cassette, Em^R	This study, deletion cassette targets entire LRΦ2 and *attB2*	pVPL3593
pVPL3002::*attB1* recovery cassette, Em^R	This study, for *attB1* recovery on ΔLRΦ1 and Δ*attB1* background	pVPL3746
pVPL3002::*attB2* recovery cassette, Em^R	This study, for *attB2* recovery on ΔLRΦ2 and Δ*attB2* background	pVPL3749
pSIP411 derivative, P_{orfX}::*ackA*	This study, for AckA expression	pVPL31093
Sakacin P induction peptide-*based* plasmid	Sørvig et al., 2003, for controlled-gene expression	pSIP411
pSIP411::recT	van Pijkeren and Britton, 2012, for controlled-recT expression	pJP042

CONTACT FOR REAGENT AND RESOURCE SHARING

Further information and requests for resources and reagents should be directed to and will be fulfilled by the Lead Contact, Jan-Peter van Pijkeren (vanpijkeren@wisc.edu).

EXPERIMENTAL MODEL AND SUBJECT DETAILS

Bacterial Strains and Growth Conditions

The strains and plasmids used in this study are listed in Key Resources Table. All *L. reuteri* strains were cultured at 37°C in deMan Rogosa Sharpe medium (MRS, BD BioSciences) or modified MRS (mMRS) supplemented with 100 mM (monosaccharides) or 50 mM (disaccharides) carbon source(s) ± SCFAs. *Escherichia coli* and *Lactococcus lactis* strains were cultured in Lysogeny Broth (LB, Neogen) at 37°C under agitation (200 rpm) and M17 (BD) containing 0.5% (w/v) glucose at 30°C (static), respectively. If applicable, M17 broth was supplemented with 100 mM carbon source ± SCFAs. If applicable, antibiotics were added as follows: erythromycin and chloramphenicol were supplemented at 5 μg/mL for *L. reuteri* and *L. lactis* strains, rifampicin or vancomycin was supplemented at 25 μg/mL or 500 μg/mL, respectively, for *L. reuteri*. *E. coli* was grown with 300 μg/mL erythromycin and 20 μg/mL chloramphenicol.

Growth Rate

For *L. reuteri*, μ_{max} (maximum growth rate) was obtained from the slope of log growth phase (OD_{600} versus time) during 1-4 hr incubation at 37°C in mMRS.

Mice

Ethics Statement

All mouse experiments were performed in accordance with NIH guidelines, Animal Welfare Act, and US federal law and were approved by the Application Review for Research Oversight at Wisconsin (ARROW) committee and overseen by the Institutional Animal Care and USE Committee (IACUC) under protocol ID A005821-A03. All mice were housed in an animal research facility (Biochemistry B145) at the University of Wisconsin accredited by the Association of Assessment and Accreditation of Laboratory Animal Care (AAALAC) International.

Mouse Strain and Husbandry

Six-week old male B6 mice (C57BL/6J) were purchased from Jackson Labs (Bar Harbor, ME). After arrival, animals were adjusted for one week to the new environment prior to the start of the experiment. Animals were housed at an environmentally controlled facility with a 12-hr light and dark cycle. Food (standard chow, LabDiet 5008, St Louis, MO) and water were provided *ad libitum*.

METHOD DETAILS

Reagents and Enzymes

DNA fragments were cloned by ligation cycle reaction (LCR) (de Kok et al., 2014). Prior to electroporation, LCR reactions were precipitated with Pellet Paint (Novagen). For cloning purposes or screen purposes, we used Phusion Hot Start Polymerase II (Thermo Scientific) or Taq polymerase (Denville Scientific), respectively. For standard ligations, we used T4 DNA ligase (Thermo Scientific). Oligonucleotides and synthetic double-stranded DNA fragments were synthesized by Integrated DNA Technologies (IDT), and are listed in Table S1.

Mitomycin C Induction

Overnight cultures of *L. reuteri* were transferred to OD_{600} = 0.1 in 40 mL pre-warmed commercial MRS. At OD_{600} = 0.2-0.3, mitomycin C (0.5 μg/mL) was added, and we determined the OD_{600} every hour for up to 8 hr (Figure S1A). Subsequently, we harvested the bacterial supernatants containing presumptive phages by centrifugation (1 min at 5,000 rpm), followed by filtration (0.22 μm PVDF, Millipore).

Identification of Prophages in *L. reuteri* 6475

Prophages in *L. reuteri* genomes were identified using the PHAge Search Tool (PHASTER) (Arndt et al., 2016). To accomplish this, the *L. reuteri* 6475 genome sequence, retrieved from the databases Integrated Microbial Genomes (IMG) at Joint Genome Institute (JGI), were uploaded to PHASTER followed by standard PHAST prophage analysis.

Identification of Prophage Excision and *attB* Sites in *L. reuteri* 6475

At OD_{600} = 0.2-0.3, *L. reuteri* 6475 was transferred to a deep-well 96-well plate (46 wells, 1 mL/well). Half of the cultures (n=23) were induced with mitomycin C (0.5 μg/mL) and cultured for 3 hr. By PCR on cell pellets of each of the cultures, we determined the proportion of integrated or excised prophages: oligonucleotides oVPL3148-3149-1439 and oVPL3150-1440-1586 were used to identify integration/excision of LRΦ1 and LRΦ2, respectively (Figures S1B and S1C, and Table S1). From mitomycin C induced cultures (as above), PCR amplicons were generated with oligonucleotide pairs oVPL1437-oVPL1439 and oVPL1440-oVPL1441, which flank prophage #1 and prophage #2, respectively. These were subjected to Sanger sequencing (GeneWiz) to determine the *attB* sites based on the presence of palindrome repeats and comparison to the integrated prophage genome sequences (Figure S1B).

Phage Production in Media with Different Carbohydrates

Sixteen-hour cultures of *L. reuteri* 6475 were washed once with same volume of basal MRS (bMRS) and resuspended in equal volume of bMRS. Subsequently, the cell suspension was inoculated into 10 mL mMRS (OD_{600} = 0.1) containing 100 mM monosaccharide (arabinose, or galactose, or glucose, or xylose, or fructose) or 50 mM disaccharide (maltose). Following 24 hr incubation at 37°C, cell-free supernatants were prepared by centrifugation (1 min at 5,000 rpm), followed by filtration (0.22 μm PVDF, Millipore). All samples were subjected to plaque assay for enumerating phages.

For *Lactococcus lactis* NZ9000::ΦTP901 by using *Lactococcus lactis* 3107 as a phage host strain, a 16 hr culture was washed once in M17, and resuspended in equal volume of M17. Subcultures were prepared as described above with the only difference that the medium was M17. Following 24 hr culture at 30°C, cell-free supernatants were prepared as described above.

Construction of Prophage Deletion Strains

Construction of LRΔΦ1ΔattB1

To delete prophages in *L. reuteri*, we used the recently in-house developed counter-selection plasmid pVPL3002 that is broadly applicable in lactobacilli (Zhang et al., 2018). First, we deleted each prophage including the *attB* sites. Briefly, LCR was used to clone the upstream and downstream flanks of each prophage in pVPL3002 to yield pVPL3590 to delete prophage #1 (see Table S1 for oligonucleotides). First, we deleted prophage #1: 5 μg pVPL3590 was electroporated in *L. reuteri* 6475 as described previously (Zhang et al., 2018), followed by recovery in MRS and plating on MRS agar containing 5 μg/mL erythromycin. Erythromycin resistant (Em^R) colonies were screened by colony PCR to confirm single-crossover homologous recombination using oligonucleotides

oVPL49-1436-1439 and oVPL97-1436-1439 for upstream and downstream integration of pVPL3590. Upon confirmation of single-crossover homologous recombination, a single colony was cultured in MRS for 20 generations and plated on MRS agar containing 500 μg/mL vancomycin, which yields only colonies after a second homologous recombination event. Deletion of LRΔΦ1Δ*attB1* was confirmed with oligonucleotides oVPL1436-oVPL1439, and the strain was named VPL4079 (*L. reuteriΔΦ1ΔattB1*).

Construction of LRΔΦ2ΔattB2

To delete prophage #2 and its *attB* site, LCR was used to clone the upstream and downstream flanks of prophage in pVPL3002 to yield pVPL3593 (see Table S1 for oligonucleotides). We transformed 5 μg pVPL3593 in *L. reuteri* 6475, and identified upstream and downstream recombinants in an identical manner as described for the construction of VPL4079. We used oligonucleotide pairs oVPL49-1585-1586 and oVPL97-1585-1586 to identify upstream and downstream integration of pVPL3593, respectively. Upon confirmation of single-crossover homologous recombination, a single colony was cultured and plated in an identical manner as described for VPL4079. Deletion of prophage #2 and its *attB* site was confirmed with oligonucleotides oVPL1585-oVPL1586, and the strain was named VPL4104 (*L. reuteriΔΦ2ΔattB2*), which we confirmed could be used as a host for LRΦ2.

Construction of LRΔΦ1ΔΦ2ΔattB1ΔattB2

To generate a double prophage-deletion variant lacking both prophages and their corresponding *attB* sites, we used VPL4079 (LRΔΦ1Δ*attB1*) as our genetic background and deleted LRΦ2 and its *attB* site in an identical manner as described above to yield strain VPL4090 (*L. reuteriΔΦ1ΔΦ2ΔattB1ΔattB2*), which serves as a host to form plaques upon exposure to LRΦ1 or LRΦ2.

attB Recovery of LRΔΦ1ΔΦ2ΔattB1ΔattB2

We restored the *attB* sites of each phage to yield a genotype that is identical to when the phage would naturally excise from the genome. Cell pellets derived from mitomycin C induced wild-type cells were used as a template for PCR to amplify the *attB1* recovery cassette (oVPL1516-1519) and *attB2* recovery cassette (oVPL1528-1531). Each recovery cassette was cloned into the pVPL3002 by LCR with bridging oligonucleotides oVPL1520 and oVPL1522 (*attB1*) to yield pVPL3746 and pVPL3749. In an identical manner as described above, we restored the *attB* sites by two-step homologous recombination in VPL4090. To identify single-crossover and double-crossover recombination, we used the same oligonucleotides as for the construction of VPL4079 and VPL4104. The resultant double-crossover recombinant was named VPL4121 (*L. reuteri*ΔΦ1Φ2).

Plaque Assay for *L. reuteri* 6475 Phages

Strains VPL4090 (*L. reuteri*ΔΦ1Δ*attB1*ΔΦ2Δ*attB2*) and VPL4104 (*L. reuteri*ΔΦ2Δ*attB2*), hereafter referred to as the LH (universal) and LH2 (LRΦ2-specific), respectively, formed plaques when exposed to supernatant derived from mitomycin C induced *L. reuteri* 6475 cultures. For plaque assays, culture supernatants were filter-sterilized (0.22 μm, Millipore) and serial dilutions were performed in phage diluent (8.0 mM $MgSO_4$ and 10.0 mM Tris-HCl, pH 7.5). An overnight culture of the LH was washed once with one volume of phage diluent, and adjusted to OD_{600} = 2.0 in phage diluent. The diluted supernatants (200 μL) were mixed with 200 μL LH cell suspension and 4 μL 1 M $CaCl_2$ solution followed by 1 hr incubation at 37°C. Subsequently, 3 mL soft top-agarose solution (0.2%, w/v) containing 10 mM $CaCl_2$ (heated to 50°C) was gently added into the mixture followed by pouring on a MRS-agar plate containing 10 mM $CaCl_2$. Plates were incubated overnight at 37°C.

Construction of Rifampicin-Resistant Derivatives and Inactivation of *ackA*, *recA*, and *mdh*

We used single-stranded DNA recombineering (SSDR) to yield rifampicin-resistant derivatives, and to inactivate the acetate kinase gene (*ackA*), the recombinase gene (*recA*), and the mannitol dehydrogenase gene (*mdh*) in an identical manner as described before (Oh and van Pijkeren, 2014). *L. reuteri* 6475 harboring pJP042—producing RecT upon induction (van Pijkeren and Britton, 2012) were transformed with 100 μg oVPL236, oVPL2870, oVPL2862 or oVPL3135 to modify *rpoB*, *ackA*, *recA* or *mdh*, respectively. To identify *rpoB* recombinants, we plated cells on MRS containing 25 μg/mL rifampicin. The genotype of the rifampicin-resistant colonies was confirmed by mismatch amplification mutation assay (MAMA) PCR (Alonso et al., 2005) using oligonucleotide combination oVPL304-305-306. Upon transformation of the other oligonucleotides, bacteria were plated on MRS plates without antibiotic selection, and colonies were screened with MAMA-PCR using oligonucleotides oVPL2871-2872-2873, oVPL2863-2864-2864 and oVPL3136-3137-3138 to identify recombinant *ackA*, *recA* and *mdh*, respectively. Pure genotypes were obtained following streak plating, which was confirmed by PCR using the same oligonucleotides, and by Sanger sequencing.

Complementation of *ackA*

By blunt-end ligation we cloned the *ackA* gene (oVPL2972-2973) in the pSIP411 backbone (oVPL399-2971) (Sørvig et al., 2005). The resultant construct (pVPL31093) was transformed in *L. reuteriΔackA* and referred to as COMP. Control strains were *L. reuteri* wild-type (WT) and *L. reuteriΔackA* transformed with pSIP411, which are referred to as WT-ctrl and Δ*ackA*-ctrl. For complementation studies, we cultured strains for 24 hr in mMRS with 100 mM glucose, after which cells were sub-cultured to OD_{600} = 0.1 in mMRS containing glucose and 10 ng/mL induction peptide (see Key Resources Table).

In Silico Analysis to Map the Central Metabolism in *L. reuteri* 6475

Enzymes involved in glucose-, fructose-, pentose-phosphate-, acetogenenic-, citric acid, and C4-metabolism were initially identified with the Kyoto Encyclopedia of Genes and Genomes (KEGG) tool; the genome of *L. reuteri* JCM 1112, which only shows a few SNPs difference to strain 6475 (Walter et al., 2011), was initially used as a reference to determine the presence of enzymes involved in the respective pathway followed by BLASTN and BLASTP search against *L. reuteri* 6475 genome (Figure 3A and Table S2). Enzymes of

L. reuteri 6475 missing in KEGG pathways were manually determined through homolog search in the non-redundant database of NCBI using BLASTP and/or PSI-BLAST. Functional domains in the putative enzymes were predicted by searching the protein families database (Pfam, http://pfam.xfam.org/).

Metabolic End-Product Analysis

For all end-product analyses, *L. reuteri* and its derivatives were cultured for 16 h in mMRS containing 100 mM glucose. Cell pellets were washed once in bMRS, which lacks carbon source, and sub-cultured to OD_{600} = 0.1 in mMRS supplemented with select carbon sources. bMRS was supplemented with one of the following: 100 mM glucose, 100 mM fructose, different ratios of glucose:fructose, 100 mM glucose and short-chain fatty acids. For SCFA supplementation, we added acetic acid—ranging from 10-60 mM or 100 mM, butyric acid (100 mM), propionic acid (100 mM), or 100 mM of a 60:20:20 mixture of acetic:propionic:butyric acids in mMRS supplemented with 100 mM glucose. In experiments where we supplemented mMRS with SCFAs, the medium was adjusted to pH 6.5, and filter sterilized (0.22 μm, PVDF, Millipore) prior to inoculation. All cultures were incubated for 24 hr, after which we determined the cell density (OD_{600}). We generated cell-free supernatants by filter-sterilization (0.22 μm, PVDF, Millipore) and tested for the presence of glucose, fructose, L-lactic acid, D-lactic acid, ethanol, and acetic acid using an enzymatic assay as per manufacturer instructions (R-Biopharm). Supernatants were also used to determine phage numbers as described above.

L. reuteri Survival and Phage Production during GI Transit in Mice

Individually caged mice (n = 5/bacterial strain) were gavaged for two consecutive days with 100 μL PBS suspension containing 10^9 CFU of rifampicin-resistant *L. reuteri* 6475 (VPL4126) or *L. reuteri*ΔΦ1ΔΦ2 (VPL4129). Whole fecal samples were collected from the bedding 16 hr after the last oral administration, and animals were sacrificed. Cecal and colon contents were harvested and weighted. Fecal, cecal and colon materials were resuspended in PBS to 100 mg/mL, and plated on MRS-agar plates containing 25 μg/mL rifampicin. The fecal suspension was also used to determine the PFU/ml by a plaque assay.

Two-Arm Dietary Crossover Study

Mice (n = 24) were individually housed as described above. Per treatment group, we included 6 animals: i) Glucose and *L. reuteri* wild-type; ii) Fructose and *L. reuteri* wild-type; iii) Glucose and *L. reuteri*Δ*ackA*, and iv) Fructose and *L. reuteri*Δ*ackA*. At day 0, all mice had *ad libitum* access to drinking water containing either glucose or fructose (14 mg/mL). At days 1-7 animals were gavaged daily with 10^9 CFU while continuing to have unlimited access to the sugar-supplemented drinking water, followed by seven days wash-out during which the animals received regular drinking water and were not subjected to gavage. After 7 days, we confirmed that we could not detect either *L. reuteri* or its phages from the fecal material. Then, the treatments were reversed, and the mice were again gavaged with *L. reuteri* for 8 days. Daily, 16 hr following the gavage, fresh fecal pellets were collected, which were subjected to bacterial CFU counts, viral plaque counts, and acetic acid analysis. Bacterial and viral loads were determined as described above. Acetic acid levels were determined in the fecal suspension using an enzymatic assay to detect analytes in complex matrices (R-BioPharm).

QUANTIFICATION AND STATISTICAL ANALYSIS

Statistics

Graphs were prepared in DataGraph 4.3 (Visual Data Tools, Chapel Hill, North Carolina, United States, https://www.visualdatatools.com). Statistical comparisons were performed using paired t test, one-way ANOVA, and Tukey's HSD (JMP Pro, version 11.0.0). For Pearson correlation and p value we performed multivariate pairwise correlations (JMP pro 11.0.0). Five mice per group (n = 5) were used for the analysis of *L. reuteri in vivo* survival and phage production in cecum, colon, and feces (Figure 1) and six mice per group (n = 6) were used for the *in vivo* two-arm dietary crossover study (Figures 2F, 2G, and 5). To analyze statistical significance of *in vivo* crossover study, we used a linear mixed effect model (Milliken and Johnson, 2001) (SAS 9.4). Three biological replicates were performed for all *in vitro* studies and statistical significance was denoted by * ($p < 0.05$), ** ($p < 0.01$), or *** ($p < 0.001$). All samples were included in the analyses, and experiments were performed without blinding.

DATA AND SOFTWARE AVAILABILITY

The genome in the NCBI database reported in this paper are GenBankcession: GCA_0000159475.2 (*L. reuteri* ATCC PTA 6475); GenBank assembly accession: GCA_000159455.2. (*L. reuteri* ATCC 55730); GenBank assembly accession: GCA_000838065.1 (*L. lactis* ΦTP901); GenBank accession: MH837542 (*L. reuteri* ATCC PTA 6475 LRΦ1); GenBank accession: MH837543 (*L. reuteri* ATCC PTA 6475 LRΦ2).

Cell Host & Microbe, Volume *25*

Supplemental Information

Dietary Fructose and Microbiota-Derived Short-Chain Fatty Acids Promote Bacteriophage Production in the Gut Symbiont *Lactobacillus reuteri*

Jee-Hwan Oh, Laura M. Alexander, Meichen Pan, Kathryn L. Schueler, Mark P. Keller, Alan D. Attie, Jens Walter, and Jan-Peter van Pijkeren

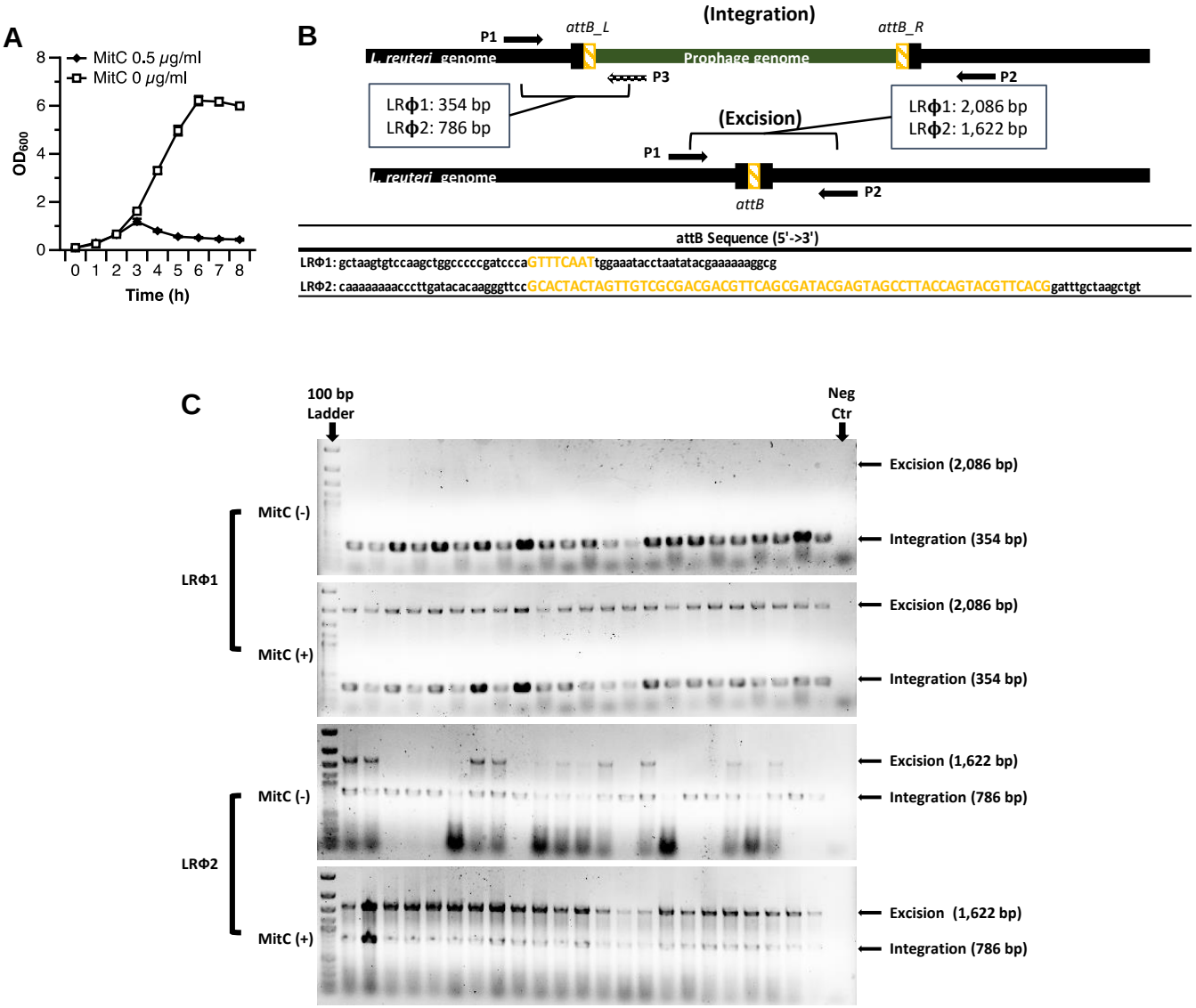

Figure S1. Related to STAR Methods | *Lactobacillus reuteri* 6475 encodes two biologically active prophages.

(A) Growth of *L. reuteri* wild-type in MRS at 37ºC for eight hours; Mitomycin C (0.5 μg/ml) was added after 1 h and the cell density (OD600) was measured every hour.
(B) Oligonucleotide design to detect integrated or excised prophage genomes, and the identified *attB* sequences (yellow) specific for LRΦ1 and LRΦ2.
(C) PCRs with oligonucleotide pairs P1-P3 and P1-P2 to determine prophage integration or excision, respectively, using cell pellets derived from 24h cultures of *L. reuteri* 6475 (MitC-) or *L. reuteri* 6475 exposed to mitomycin C (MitC+).

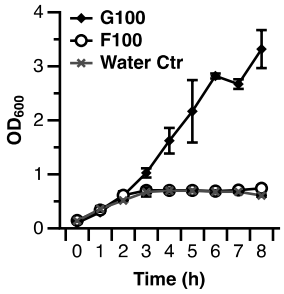

Figure S2. Related to Figure 2B | *Lactobacillus reuteri* 6475 cannot utilize fructose as a sole carbon source.

Basal MRS lacking carbon source was supplemented with water (water Ctrl), 100 mM glucose (G100) or fructose (F100). Media were inoculated with pre-washed *L. reuteri* cells to OD600 = 0.1, and growth was monitored hourly for eight hours at 37℃. Data shown are averages of 3 biological replicates and error bars represent standard deviation.

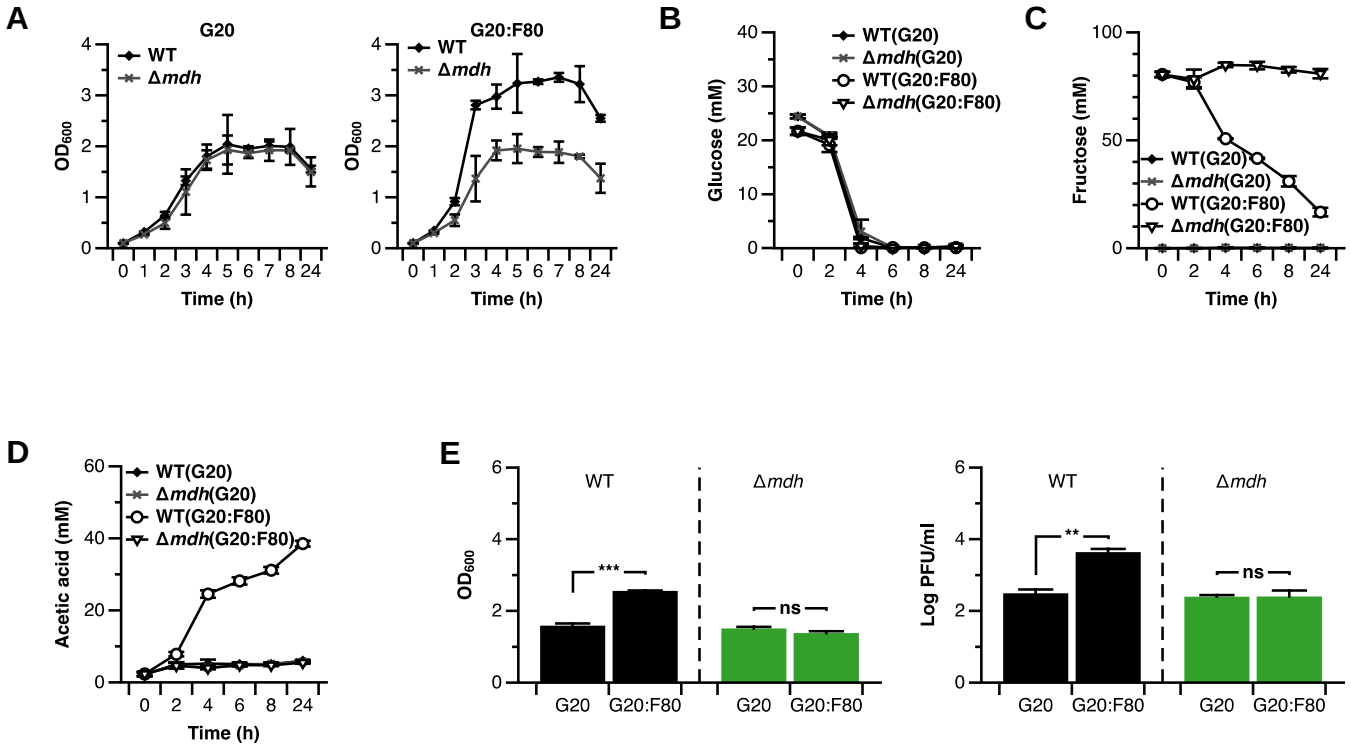

Figure S3. Related to Figure 3 | *Lactobacillus reuteri* 6475 metabolizes fructose via mannitol dehydrogenase pathway.

(A) Growth curve of WT and Δ*mdh* in bMRS containing 20 mM glucose (left, G20) and 20 mM Glucose with 80 mM fructose (right, G20:F80).

(B-D) Glucose and fructose metabolism of *L. reuteri* WT and Δ*mdh* upon 24 h growth in bMRS containing G20 and G20:F80. (B) Consumption of glucose. (C) Consumption of fructose. (D) Production of acetic acid.

(E) Final cell density and phage production of *L. reuteri* WT and Δ*mdh* after 24 h growth in in bMRS containing G20 and G20:F80. All cultures were incubated at 37℃ for 24 h. Data shown represent three biological replicates and error bars represent standard deviation.

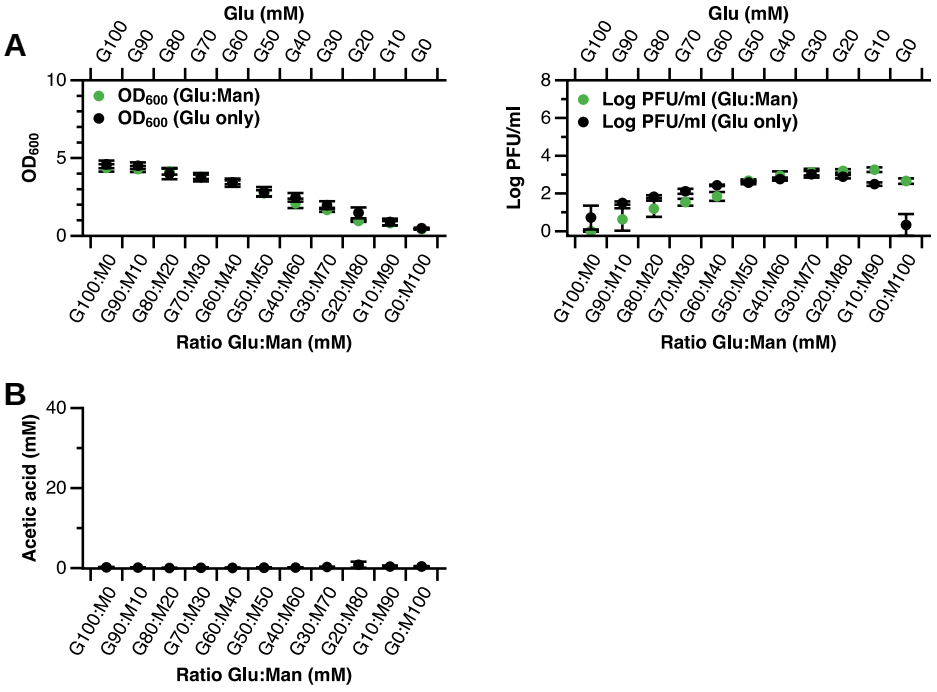

Figure S4. Related to Figure 3 | Mannitol does not contribute to *Lactobacillus reuteri* 6475 bacteriophage production.

(A) Final cell density (right) and phage production (left) following 24 h growth in 100 mM carbon source containing different ratios (mM) of glucose (Glu) and mannitol (Man) (green, primary x-axis) and different concentration (mM) of glucose (Glu) (black, secondary x-axis).

(B) Acetic acid production after 24 h growth in 100 mM carbon source containing different ratios (mM) of glucose (Glu) and mannitol (Man) at 37°C for 24 h. Data shown are averages of 3 biological replicates and error bars represent standard deviation.

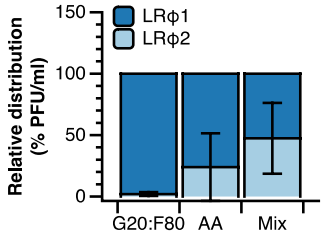

Figure S5. Related to Figure 2C and 6E | *Lactobacillus reuteri* 6475 produces LRΦ1 and LRΦ2 in mMRS supplemented with fructose, acetic acid and SCFAs mix.

L. reuteri wild-type (WT) was cultured in mMRS supplemented with 20 mM glucose and 80 mM fructose (G20:F80), mMRS containing 100 mM glucose and 100 mM acetic acid (AA), or mMRS containing 100 mM glucose and 100 mM SCFA-mix: 60:20:20 mM acetic:propionic:butyric acids (Mix) at 37℃ for 24 h, after which ratio of LRΦ1 and LRΦ2 in the culture supernatant were determined by plaque assays using universal lytic host and LRΦ2-specific lytic host. Error bars are standard deviation. Data shown are based on 3 biological experiments.

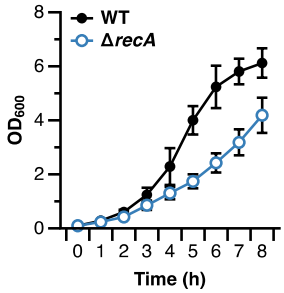

Figure S6. Related to Figure 7A | *L. reuteri*ΔrecA reduces growth rate compared to *L. reuteri* 6475 wild-type.
L. reuteri 6475 (WT) and *L. reuteri*Δ*recA* were cultured in bMRS supplemented with 100 mM glucose at 37℃ and cell density (OD_{600}) were measured every hour during eight hours incubation. Error bards are standard deviation. Data shown are based on 3 biological experiments.

Table S1. Related to STAR Methods. Oligonucleotides used in this study.

Oligo Name	Sequence (5' -> 3')	Description
oVPL49	acaatttcacacaggaaacagc	Oligo paired with oVPL97 used for screening pVPL3002 constructs
oVPL97	cccccattaagtgccgagtgc	Oligo paired with oVPL49 used for screening pVPL3002 constructs
oVPL187	taccgagctcgaattcactgg	Rev, internal oligo for pVPL3002 backbone amplification
oVPL188	atcctctagagtcgacctgc	Fwd, internal oligo for pVPL3002 backbone amplification
oVPL236	tcaaaccaccaggaccaagcgctgaaagacgacgctttc tgcttaattcacctaatgggttggtttgatccatgaactgg	Recombineering oligo targeting *Lr* VPL1014 *rpoB* gene
oVPL304	aacagcttgccgttgcatgttagc	Oligo paired with oVPL305, oVPL306 for MAMA PCR screening of Lr VPL1014 *rpoB* recombinants
oVPL305	aaaagggtgatacggtaaccaagg	Oligo paired with oVPL304, oVPL306 for MAMA PCR screening of Lr VPL1014 *rpoB* recombinants
oVPL306	aagcgctgaaagacgacgctttctg	Oligo paired with oVPL304, oVPL305 for MAMA PCR screening of Lr VPL1014 *rpoB* recombinants
oVPL399	ggctaaaatctccttgtaatagtattttatag	Fwd, pSIP411 backbone
oVPL659	tgccccgttagttgaagaag	Fwd, screening oligo for pSIP411 constructs
oVPL660	attctgctcccgcccttatg	Rev, screening oligo for pSIP411 constructs
oVPL1377	tgcccgtaatttgcgagttc	Fwd, internal of *recT1* in *LRΦ1*
oVPL1378	acaggttgccaatcctctttg	Rev, internal of *recT1* in *LRΦ1*
oVPL1379	gctagaaacgggttgccaat	Fwd, internal of *recT2* in *LRΦ2*
oVPL1380	tctacctgctgatgttatggga	Rev, internal of *recT2* in *LRΦ2*
oVPL1436	aggattccgacaacgtgact	Fwd, screening oligo paired with oVPL1438 used for screening LRΦ1 excision after MitC induction, Fwd, for SCO and DCO screening of *LRΦ1*deletion
oVPL1437	agtagcgacggcgattaaga	Fwd, screening oligo paired with oVPL1439 used for screening LRΦ1 excision after MitC induction
oVPL1438	tatgctgcgctcagtaatgg	Rev, screening oligo paired with oVPL1436 used for screening LRΦ1 excision after MitC induction
oVPL1439	atctgccattgttgctttcc	Rev, screening oligo paired with oVPL1437 used for screening LRΦ1 excision after MitC induction, Rev, oligo SCO and DCO screening of LRΦ1 deletion
oVPL1440	agatgttatttcagcggtggcg	Fwd, screening oligo paired with oVPL1441 used for screening LRΦ2 excision after MitC induction
oVPL1441	aatgccacgaggattgatcggg	Rev, screening oligo paired with oVPL1440 used for screening LRΦ2 excision after MitC induction
oVPL1442	acttaaaaactgagcagcaattgc	sequencing oligo starting 49 bases d/s of oVPL1440
oVPL1443	attataactccaatataattttcgcgc	sequencing oligo starting 398 bases d/s of oVPL1440
oVPL1444	ttggaacaaagtgaaggtctttaattgc	sequencing oligo starting 53 bases d/s of oVPL1436
oVPL1445	ataattgagttactaccaaattggtgagc	sequencing oligo starting 522 bases d/s of oVPL1436
oVPL1446	aaacggagataccgaatttaggc	sequencing oligo starting 41 bases d/s of oVPL1437
oVPL1516	aattggtgagccattggaac	Fwd, 978 bp 5' upstream flanking sequence of LRΦ1 omitting *attB1L* sequence
oVPL1517	tgggatcgggggccagcttggac	Rev, 978 bp 5' upstream flanking sequence of LRΦ1 omitting *attB1L* sequence
oVPL1518	tgtaagtggtaagccgagtaac	Fwd, 1,257 bp 5' downstream flanking sequence of LRΦ1 omitting *attB1R* sequence
oVPL1519	tggctcaacaagacacaagc	Rev, 1,257 bp 5' downstream flanking sequence of LRΦ1 omitting *attB1R* sequence
oVPL1520	aaacgacggccagtgaattcgagctcggtaaattggtgag ccattggaacaacaagcccg	Bridging oligo for LCR assembly to construct pVPL3590
oVPL1521	gctaagtgtccaagctggcccccgatcccatgtaagtggta agccgagtaacaaaccaat	Bridging oligo for LCR assembly to construct pVPL3590
oVPL1522	aaccttatctgcttgtgtcttgttgagccaatcctctagagtcg acctgcaggcatgcaa	Bridging oligo for LCR assembly to construct pVPL3590
oVPL1528	atcgcagccttaaggaaatg	Fwd, 1,217 bp 5' upstream flanking sequence of LRΦ2 omitting *attB2L* sequence
oVPL1529	agaagtaccggcatgcaaag	Rev, 1,217 bp 5' upstream flanking sequence of LRΦ2 omitting *attB2L* sequence
oVPL1530	accagtacgttcacgtaagtag	Fwd, 1,139 bp 5' downstream flanking sequence of LRΦ2 omitting *attB2R* sequence
oVPL1531	gatgcgattgcggctaatac	Rev, 1,139 bp 5' downstream flanking sequence of LRΦ2 omitting *attB2R* sequence
oVPL1532	aaacgacggccagtgaattcgagctcggtaatcgcagcct taaggaaatgggagactttt	Bridging oligo for LCR assembly to construct pVPL3593
oVPL1533	actgaatccactttgcatgccggtacttctaccagtacgttca cgtaagtagtagagctt	Bridging oligo for LCR assembly to construct pVPL3593
oVPL1534	cgtttcagcggtattagccgcaatcgcatcatcctctagagt cgacctgcaggcatgcaa	Bridging oligo for LCR assembly to construct pVPL3593
oVPL1585	cgaatcgaccctgctaagtt	Fwd, oligo SCO and DCO screening of LRΦ2 deletion
oVPL1586	gccttaactggtgggtttga	Rev, oligo SCO and DCO screening of LRΦ2 deletion, Rev primer paired with oVPL1440 and 3150 for screening LRΦ2 excision
oVPL2862	tatcaccatcaatttcagcacgaggaactaatgctgcttagc tatcaacaattactaagtcaactgctccacttgaaatc	Recombineering oligo targeting *Lr* VPL1014 *recA* gene
oVPL2863	aagatcgaaaagaacttcggtaagg	Oligo paired with oVPL2864, oVPL2865 for MAMA screening of *Lr* VPL1014 *recA* recombinants
oVPL2864	acgaggaactaatgctgcttagct	Oligo paired with oVPL2863, oVPL2865 for MAMA screening of *Lr* VPL1014 *recA* recombinants
oVPL2865	accggtcttaccactggctttatc	Oligo paired with oVPL2863, oVPL2864 for MAMA screening of *Lr* VPL1014 *recA* recombinants
oVPL2870	ttcctaacatttccgcagcacgtgcagatacataacgtcag gaggtaccgtgagcaccgtacttacgagcaccatacttc	Recombineering oligos targeting *Lr* VPL1014 *ackA* gene
oVPL2871	acgtgcagatacataacgtcagg	Primer paired with oVPL2872, oVPL2873 for MAMA screening of *Lr* VPL1014 *ackA* recombinants
oVPL2872	aattgcagttaacgctggtagttcaacac	Primer paired with oVPL2871, oVPL2873 for MAMA screening of *Lr* VPL1014 *ackA* recombinants
oVPL2873	atcatcggcggaaaggtcacgttc	Primer paired with oVPL2871, oVPL2872 for MAMA screening of *Lr* VPL1014 *ackA* recombinants
oVPL2971	gaattcggtaccccgggttcgaagg	Rev, pSIP411 backbone, oVPL399 was used as Fwd oligo for pSIP411 backbone
oVPL2972	atgtcaaaaacaattgcagttaacgc	Fwd, *ackA* (LAR_0543)
oVPL2973	ttagttatttttctttaagcgttcaatgtc	Rev, *ackA* (LAR_0543)
oVPL3135	agaccagcatagagtgccttatcagtaccacaaatacctta tcaggcagtgtgaattaagacttcatcaggcttaatttc	Recombineering oligo targeting *mdh*
oVPL3136	cgttataacagccgtttgga	Primer paired with oVPL3137, oVPL3138 for MAMA screening of *Lr* VPL1014 *mdh* recombinants
oVPL3137	cagtaccacaaatacctact	Primer paired with oVPL3136, oVPL3138 for MAMA screening of *Lr* VPL1014 *mdh* recombinants
oVPL3138	gcaaaccaacagcttcaaca	Primer paired with oVPL3136, oVPL3137 for MAMA screening of *Lr* VPL1014 *mdh* recombinants
oVPL3148	caacgccgaccaaacttatt	Fwd primer for screening LRΦ1 internal, paired with oVPL3149, oVPL1439
oVPL3149	tgaagagccaaatgatgacg	Rev primer for screening LRΦ1 internal, paired with oVPL3148, oVPL1439
oVPL3150	tgcttctgatattgccaacg	Rev primer for screening LRΦ2 internal, paired with oVPL1440, oVPL1586
oVPL3160	atgaaggcacttgttttaacaggt	Fwd, for amplifying mdh gene of *Lr* VPL1014
oVPL3161	ttaagcttcttcgcccaccaacct	Rev, for amplifying mdh gene of *Lr* VPL1014

oVPLxxxx: Van Pijkeren Lab oligonucleotide collection identification number; d/s: down-stream; u/s: up-stream; SCO: single crossover; DCO: double crossover; Fwd: forward; Rev: reverse; MAMA-PCR: Mismatch Amplification Mutation Assay-PCR

Table S2. Related to Figure 3A. Enzymes involved in *L. reuteri* ATCC PTA 6475 central metabolism.

Pathway	EC No.	Enzyme	Gene ID (JCM 1112)	Gene ID (6475)	Pathway
1	2.7.1.2	Glucokinase (Hexokinase)	LAR_1139	HMPREF0536_11189	Glycolysis
2	1.1.1.49	Glucose-6-phosphate 1-dehydrogenase	LAR_1653	HMPREF0536_11754	Pentose-phosphate pathway
3	1.1.1.44	6-phosphogluconate dehydrogenase	LAR_1654	HMPREF0536_11755	Pentose-phosphate pathway
4	5.1.3.1	D-ribulose-5-phosphate 3-epimerase	LAR_1100	HMPREF0536_11148	Pentose-phosphate pathway
5	4.1.2.9	Xylulose 5-phosphate phosphoketolase	LAR_1574	HMPREF0536_11675	Pentose-phosphate & acetogenesis pathway
6	1.2.1.12	Glyceraldehyde-3-phosphate dehydrogenase	LAR_0381	HMPREF0536_10422	Glycolysis
7	2.7.2.3	Phosphoglycerate kinase	LAR_0382	HMPREF0536_10423	Glycolysis
8	5.4.2.11	Phosphoglycerate mutase	LAR_0238, 0483, 0662, 0696, 0959, 1040, 1271, 1285, 1409	HMPREF0536_10158, 10259, 10314, 11067, 11616, 11686, 11719, 11832, 12096	Glycolysis
9	4.2.1.11	Enolase	LAR_0384	HMPREF0536_10425	Glycolysis
10	2.7.1.40	Pyruvate kinase	LAR_0722	HMPREF0536_10918	Glycolysis
11*	1.1.1.28	D-Lactate dehydrogenase/ D-2-hydroxyisocaproate dehydrogenase	LAR_0656, 1523	HMPREF0536_10988, 11681	Glycolysis
11	1.1.1.27	L-Lactate dehydrogenase/ L-2-hydroxyisocaproate dehydrogenase	LAR_0688, 0853, 1085, 1206, 1785	HMPREF0536_10759, 11902, 10954, 10955, 11255	Glycolysis
12	1.2.4.1	Pyruvate dehydrogenase	LAR_0608	HMPREF0536_11042	Glycolysis
13*	2.7.2.1	Acetate kinase	LAR_0543	HMPREF0536_10605	Acetogenesis **(this study)**
14*	2.3.1.8	Phosphate acetyltransferase	LAR_0393	HMPREF0536_10435	Potential acetogenesis
15*	1.2.1.3	Aldehyde dehydrogenase	LAR_1623	HMPREF0536_11724	Glycolysis (potential acetogenesis)
16	1.1.1.1	Bi-functional acetaldehyde/alcohol dehydrogenase	LAR_0310	HMPREF0536_10346	Ethanol/potential acetogenesis
16	1.1.1.1	Alcohol dehydrogenase	LAR_1406, 1444, 1489	HMPREF0536_11520, 11835, 11973	Ethanol/potential acetogenesis
17	2.2.1.6	Acetolactate synthase	LAR_0126	HMPREF0536_12082	C4 metabolism
18	4.1.1.5	Acetolactate decarboxylase	LAR_0127	HMPREF0536_12083	C4 metabolism
19	1.1.1	Acetoin reductase	LAR_1360	HMPREF0536_11434	C4 metabolism
20*	1.1.1.255	Mannitol dehydrogenase	LAR_1742	HMPREF0536_11857	Fructose metabolism
21†	2.7.1.4	Fructokinase	LAR_0854, 0855 (frame-shift mutation between LAR_0854 and 0855)	HMPREF0536_10757, 10758 (Frame-shift mutation between HMPREF0536_10757 and 10758)	Fructose metabolism
22	5.3.1.9	Glucose-6-phosphate isomerase	LAR_0415	HMPREF0536_10457	Gluconeogenesis/fructose metabolism
23	2.7.1.90	D-fructose-6-phosphate 1-phosphotransferase	N/A	N/A	Fructose metabolism
24	2.3.3.8	Citrate lyase	N/A	N/A	Citric acid utilization

Pathway numbers are corresponding to Fig. 3a.

Abbreviation of metabolic substrates are **G6P**, glucose-6-phosphate; **6PG**, 6-phosphogluconate; **R5P**, ribulose-5-phosphate; **X5P**, xylulose-5-phosphate; **GAP**, glyceraldehyde-3-phosphate; **1,3BPG**, 1,3-biphosphoglycerate; **3PG**, 3-phosphoglycerate; **2PG**, 2-phosphoglycerate; **PEP**, Phosphoenolpyruvate; **Acetyl-P**, acetyl phosphate; **F6P**, fructose-6-phosphate; $F1,6P_2$, fructose-1,6-bisphosphate.

EC, Enzyme commission Number; **Gene ID**, gene ID found in *L. reuteri* chromosome; *****, enzymes not available in KEGG pathway, but present in *L. reuteri*; **†**, genes with a frameshift mutation. *L. reuteri* JCM 1112 genome was used as a reference genome and compared with *L. reuteri* ATCC PTA 6475 genome.